NASA Contractor Report 4039

Dynamic Testing of a Two-Dimensional Box Truss Beam

Charles W. White

CONTRACT NAS1-17551
JANUARY 1987

NASA

NASA Contractor Report 4039

Dynamic Testing of a Two-Dimensional Box Truss Beam

Charles W. White

Martin Marietta Denver Aerospace
Denver, Colorado

Prepared for
Langley Research Center
under Contract NAS1-17551

National Aeronautics
and Space Administration

Scientific and Technical
Information Branch

1987

Table of Contents

List of Tables

List of Figures

Table of Contents (Continued)

Table of Contents (Continued)

1.0 SUMMARY

Testing to determine the effects of joint freeplay and pretensioning of diagonal members on the dynamic characteristics of the box truss space structure was first proposed by Martin Marietta Denver Aerospace on its Independent Research and Development (IR&D) project D-54D. A test article for this purpose was designed and built under D-54D. The test article consisted of ten bays of planar truss, each measuring 2 meters per side, suspended by long wires at each joint. Each side was made of square aluminum tubing, and all corner fittings were made of cast aluminum. Pins of varying size were used to assemble the truss thereby simulating various joint freeplay conditions. All joints could be shimmed and bolted tight to assure a no freeplay condition. Single, unloaded tube diagonals were interchangeable with dual, tensioned steel rod diagonals. Modal analyses of the suspended tube diagonal configuration were conducted under D-54D and used to calculate frequency response functions simulating proposed test conditions for the purpose of evaluating the suspension system. A preliminary single-point random excitation of the test article also was conducted for this purpose. This completed the project D-54D effort.

Martin Marietta was then awarded a contract (Task 4 of NAS 1-17551) to test the D-54D-developed test article. This document reports the results of that task. The objective of the task was to quantify the effect of joint freeplay on a multi-bay statically determinate truss, and then assess the effects when the structure is modified to incorporate pretensioned diagonals producing a statically indeterminate truss. It was also desirable to assess the effects of levels of dynamic load on the dynamic performance of the truss. Testing of four truss configurations was specified:

1. Truss with tight joints

2. Truss with joints having normal freeplay

3. Truss with joints having excessive freeplay (three times or more than normal freeplay)

4. Truss with normal freeplay and cross-tension diagonals

The effect of magnitude of dynamic load was to be assessed for each test.

Table 1 summarizes the results of these tests and presents the analytically predicted values of the first two global modes of both the tube and tension diagonal configurations.

Table 1 Summary of First and Second Global Bending Mode Frequencies

TEST CASE	CONFIGURATION DESCRIPTION	1st BENDING FREQUENCY (Hz)	2nd BENDING FREQUENCY (Hz)
	Predicted for FEM Analysis of Tube Diagonal Configuration	19.3	46.3
1.	Tube Diagonals with Tight Joints	20.0	55.84
2.	Tube Diagonals with Normal Freeplay (1 mil)	17.72	51.59
3.	Tube Diagonals with Excessive Freeplay (3 mil)	*	*
	Predicted for FEM Analysis of Tension Diagonals Configuration	17.3	53.48
4a.	Tension Diagonals with Tight Joints	16.88	*
4b.	Tension Diagonals with Normal Freeplay (1 mil)	15.47	49.75

* Could not be determined by test.

The first item in Table 1 is the analytical prediction of the 1st and 2nd global truss bending mode. These frequencies were obtained from a finite element model (FEM) reflecting the tube diagonal configuration. Program FINEL, in Martin Marietta's FORMA Library, was used to generate this FEM. All joints had 6 degrees of freedom with fixed boundaries (i.e., no pinned joints). Mass data reflected the measured weight of truss parts, including accelerometers. Many other modes were obtained from this FEM. Some of them were suspension system modes and out-of-plane modes (i.e., motion perpendicular to the direction of excitation). Many others were in-plane modes whose apparent shapes are similar to either the first or second bending modes and whose frequencies ranged anywhere from slightly above (e.g., 22.8 Hz) the first bending mode frequency to well above (e.g., 57.5 Hz) the second bending mode frequency. Review of the strain energy distribution among the elements of the model in each mode revealed that these modes were primarily local element bending (as opposed to global truss bending). This proliferation of modes exists because the pinned-pinned frequency (19.9 Hz) of every 2-meter length of truss was close to the predicted first global bending mode frequency. This condition allows the rotation of joints in the global modes to drive local bending motions. Because this phenomenon depends upon unknown and time variable boundary conditions at all joints, correlation of analyses with test results was not successful at frequencies where local/global coupling occurred. Qualitative correlation under these conditions is discussed later in this report.

As seen in Table 1, the first bending frequency of the tight joint configuration test result agrees well with the predicted value. The second mode frequency is high, but local/global coupling is the probable cause. The first measured bending frequency of the normal freeplay configuration decreased to 17.72 Hz. This value is in agreement with the modal freeplay prediction method described in the report. The second mode also decreased in frequency, but it was not possible to tell whether this was due directly to freeplay (translation effects) or due to local/global coupling changes (moment effects) associated with the change from tight to freeplay boundary conditions.

No modal characteristics could be identified when excessive freeplay was present.

Two tension diagonal configurations were tested (cases 4a and 4b of Table 1). In both cases the first bending frequency was much lower than could be justified by analysis. The predicted frequencies of the tension diagonals configuration also are shown in Table 1. The absence of any test observed second mode for case 4a could not be explained. The second bending frequency for case 4b was consistent with first mode frequency drop; but, like all second mode data results, was obfuscated by local/global coupling effects.

The following conclusions and recommendation were made:

Conclusions

- 0 The test article exhibited a multitude of local/global coupling modes.
- 0 Instrumentation was insufficient to identify all modes.
- 0 Local/global coupling prevented theoretical/experimental correlation improvement of modes that were identified.
- 0 Sufficient data were obtained to evaluate the Martin Marietta-developed modal freeplay methodology of predicting joint freeplay effects.
- 0 Assessment of the effects of pretensioned diagonals was impeded by local/global coupling effects.
- 0 Quality of test data did not allow identification of reliable modal damping values.

Recommendations

- 0 Design future large space structures (LSS) tests so that ratios of local bending frequency/global bending frequency are the same for test article and prototype.
- 0 Avoid LSS designs having local bending frequencies in the range of global modes whose shape or vibration amplitude must be controlled.

2.0 INTRODUCTION AND OBJECTIVES

The processes by which aerospace structures are sized to withstand operational loads and by which control systems are designed usually involve the calculation and use of modal characteristics of that structure. In order for this process to be valid, it is necessary that the structure behave in a reasonably linear manner over the range of operational loads, because the analysis by which modal characteristics are determined is based on the assumption of linearity. However, many large space structures (LSS) currently under consideration will be composed, in part, of truss structures of some type. These trusses will be deployable or erectable in space. Some freeplay in joints of deployable trusses may be required to permit smooth deployment using low drive force deployment mechanisms. For erectable structures, joint freeplay may be required to facilitate assembly in space. It is obvious that the presence of freeplay in joints will violate the assumption of linearity, thereby degrading the validity of analytically predicted modal characteristics to some extent. Joints having post deployment/erection tightening features to eliminate freeplay have been proposed, but the dollar and weight costs of such designs are not negligible. In order to decide whether or not these more expensive joint designs are required, it is necessary to dynamically test representative truss structures to measure the change in modal characteristics caused by joint freeplay.

Therefore, the objective of the task performed under contract NAS 1-17551 and described in this report was twofold. The primary objective was to dynamically test a planar box truss to quantify the effects of joint freeplay and member preload on the dynamic parameters. The secondary objective was to enhance the understanding of analytical methods to predict the dynamic performance of such trusses.

Contents of the report are organized in the following manner: Section 3 contains a description of the test article and the design effort accomplished under Martin Marietta Denver Aerospace Independent Research and Development Project D-54D. The analytical model generated to predict test results and for theoretical/analytical correlation studies is discussed in Section 4. A very brief description of the test setup and data reduction methods is presented in Section 5. In Section 6, the results of each test are presented and discussed. Finally, conclusions and recommendations are stated in Section 7.

3.0 DESIGN OF TEST ARTICLE

3.1 Description of Test Structures

The representative truss structure selected for test was designed and fabricated under the Martin Marietta Denver Division Independent Research and Development (IR&D) project D-54D entitled "Large Space Structures Design and Analysis." This section presents the dynamic test article progress from that IR&D project.

The truss design was a 20-meter-long planar beam made up of ten bays, 2x2 meters each (Figures 1 and 2). This beam provided a sufficient length-by-depth ratio to ensure that the test model would behave as a realistic beam (with ratios of bending and shear strain similar to actual large structures). Also, the ten bays ensured that the test article had a representative number of joints, i.e., the dynamic response of the structure would be highly dependent on joint behavior.

The test article was designed and built to have interchangeable diagonal braces, i.e., a single tension-compression member per bay making the truss statically determinate, or two tension-only members per bay making the truss statically indeterminate. In addition, the end fittings were designed to accommodate various diameters of fasteners and pins to allow the amount of freeplay in the truss to be changed. With these two design features, the test article can be modified so that five dynamic models can be tested. The models are: (1) statically determinate truss with no freeplay; (2) statically determinate truss with normal freeplay for a deployable truss, i.e., 1 to 3 mils freeplay at each joint; (3) statically determinate truss with excessive freeplay, i.e., 3 to 6 mils freeplay at each joint; (4) statically indeterminate, tension diagonal truss with no freeplay; and (5) statically indeterminate tension diagonal truss with normal freeplay.

Figures 1 and 2 show two of the dynamic test models. Figure 1 shows the dynamic test model with single diagonal braces and clamped end-fittings to assure no freeplay. Figure 2 is the dynamic test model with tensioned diagonals and end-fitting fasteners that provide between 1 and 3 mils freeplay. As shown in the figures, the test article was fabricated using component designs identical to the actual box-truss structure. However, for cost reasons, aluminum and steel were used rather than graphite/epoxy, which is planned for flight systems.

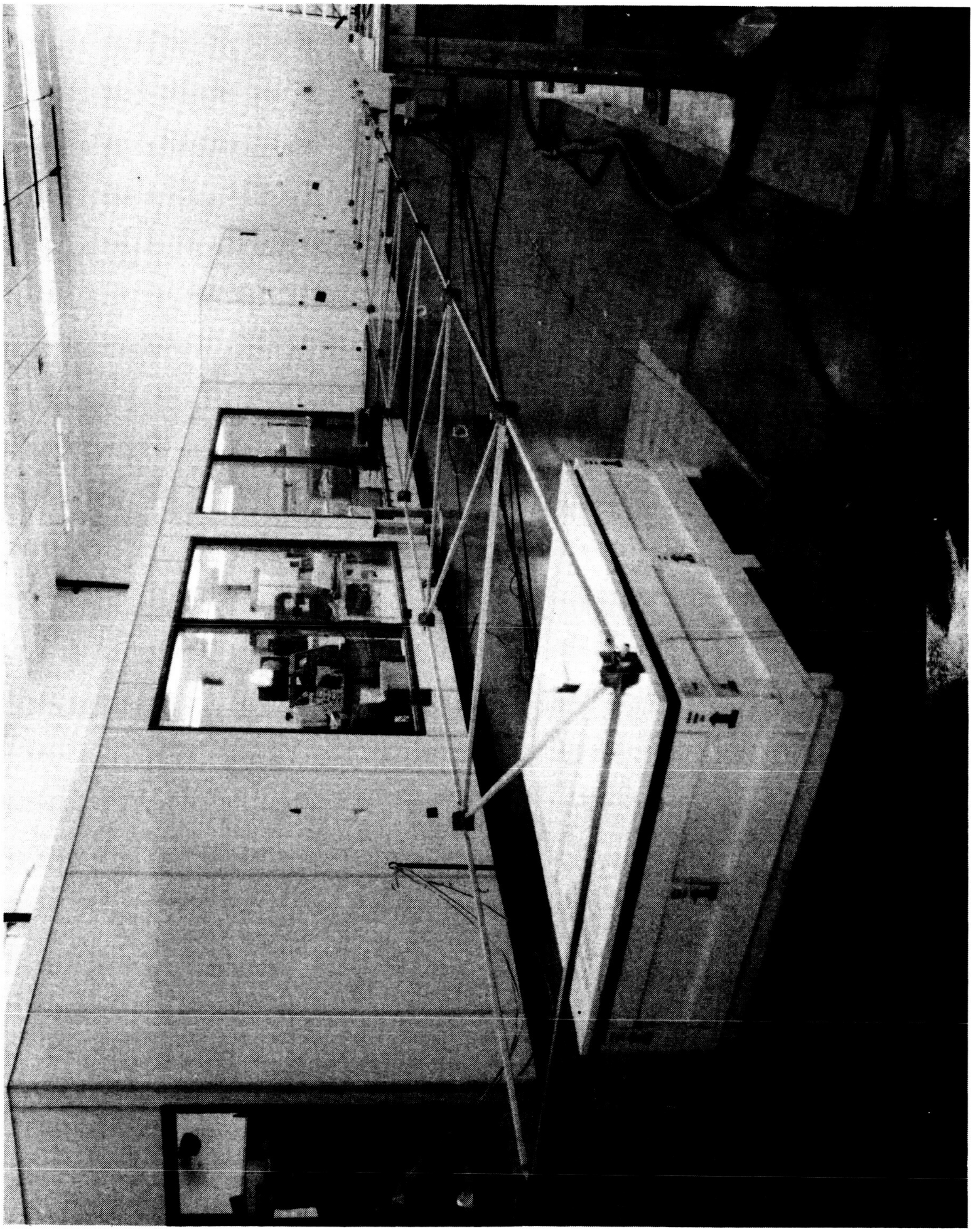

Figure 1 20-Meter Truss Model with Tube Diagonals

ORIGINAL PAGE IS
OF POOR QUALITY

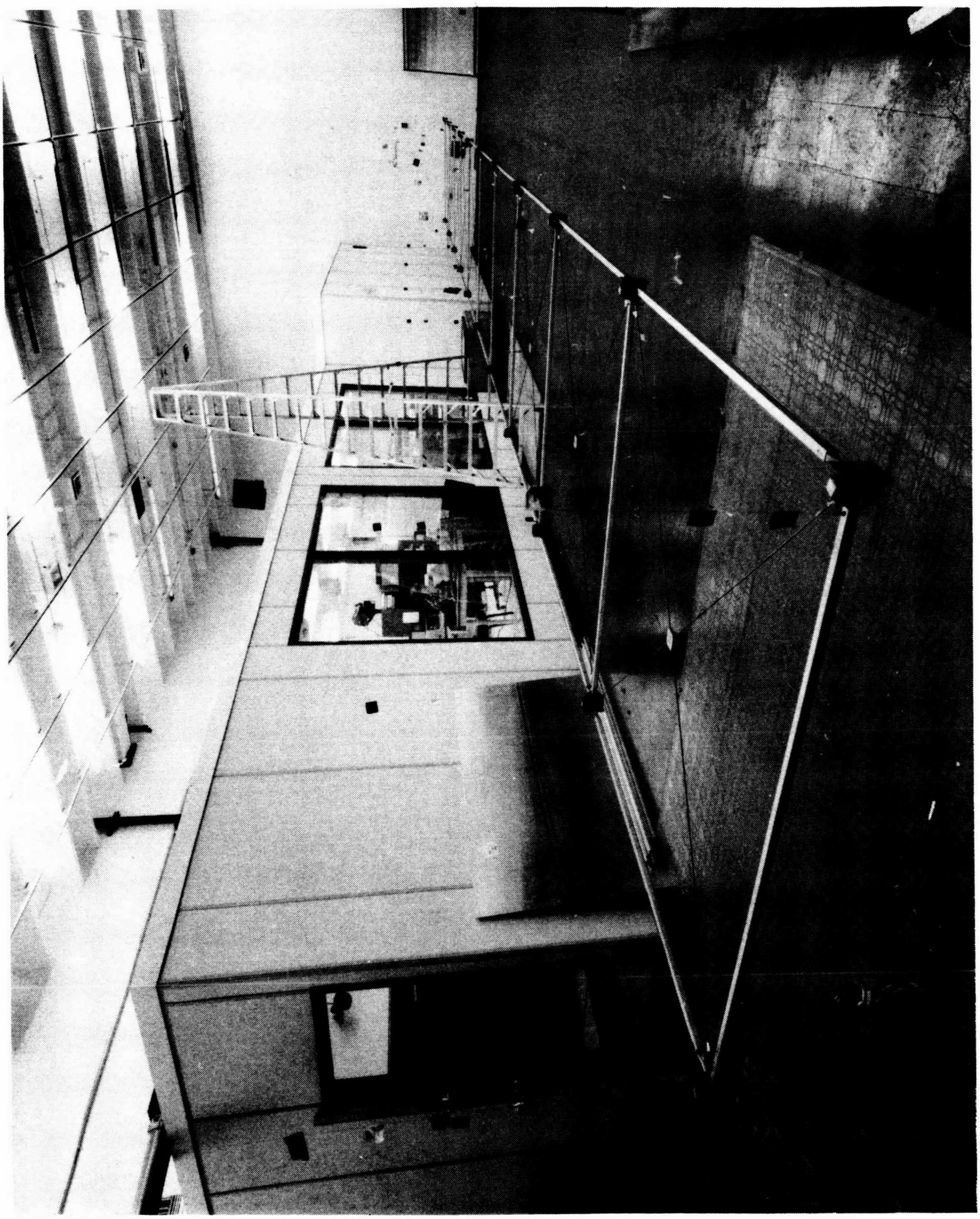

Figure 2 20-Meter Truss Model with Tensioned Diagonals

The corner fittings and end fittings are cast aluminum parts and were designed to be functionally identical to the flight design (Figure 3). The aluminum tubing is 1-inch square aluminum extrusion with 0.05-inch wall. The tension diagonals used 0.1875-inch diameter steel rod. The steel rod was sized such that the specific stiffness was approximately half that of the aluminum tubing. Therefore, the statically determinate model using a single aluminum diagonal and the statically indeterminate model using pairs of tensioned steel diagonals will have the same natural frequency. A simple and cost-effective method to allow tensioning of the steel diagonals was employed by threading opposing ends of the rods with right-hand and left-hand threads. This produced a turnbuckle type of design.

3.2 Analyses to Support Test Plan

In addition to designing and building the test article, a test plan was completed in 1985 that defined the test fixture and testing requirements to assure sufficient resolution of test measurements and to identify and characterize the frequency, mode shape and damping. This included using a finite-element analytical model and an actual random vibration test of the test article to verify the test fixture design.

To design the test fixture, the following design requirements were considered:

1) The test fixture must simulate zero-g support environment to minimize the effect of gravity on joint freeplay.

2) The test fixture must provide a method to assure the truss is planar, thereby reducing any out-of-plane motions when the truss is excited inplane.

3) The test fixture's natural frequency must be out of the range of the modal frequencies to be measured for the truss.

To meet these requirements, a suspension system of 22, 0.013-inch diameter, piano wires was chosen (one wire per corner fitting). This suspension system allows the truss to be hung parallel to the ground and provides a near zero-g support system. Making each wire approximately 15 feet long assured that the natural frequency of the suspension system was far less than the natural frequency of the truss. To assure the truss could be hung planar to within $\pm$ 0.02 inch, each piano wire was soldered to an adjustment screw (Figure 3).

Using a finite-element model of the truss, analyses of the suspension system and testing requirements were performed. The finite-element model consisted of 6-DOF beam elements to represent the aluminum truss members. The 22 corner fittings were accounted for by lumped masses at the node points. The piano wire suspension system was modeled as axial-only rod elements. Figure 4 shows the resulting model. Modifications of this initial finite-element model were made to assess truss sensitivity with respect to the following imperfections:

ORIGINAL PAGE IS
OF POOR QUALITY

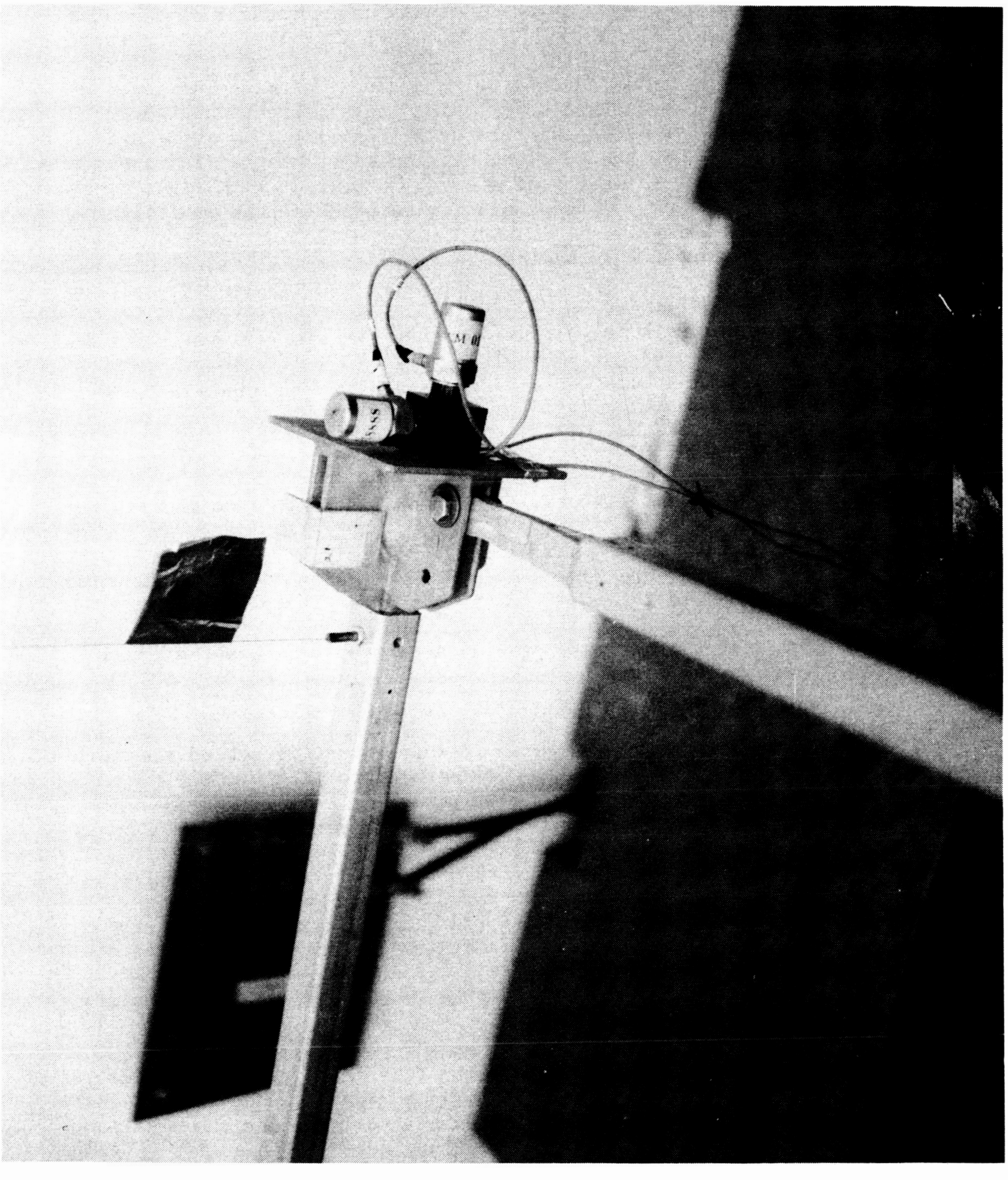

Figure 3 Corner Fitting Showing Accelerometer Placement, Theodolite Target and Adjustment Mechanism

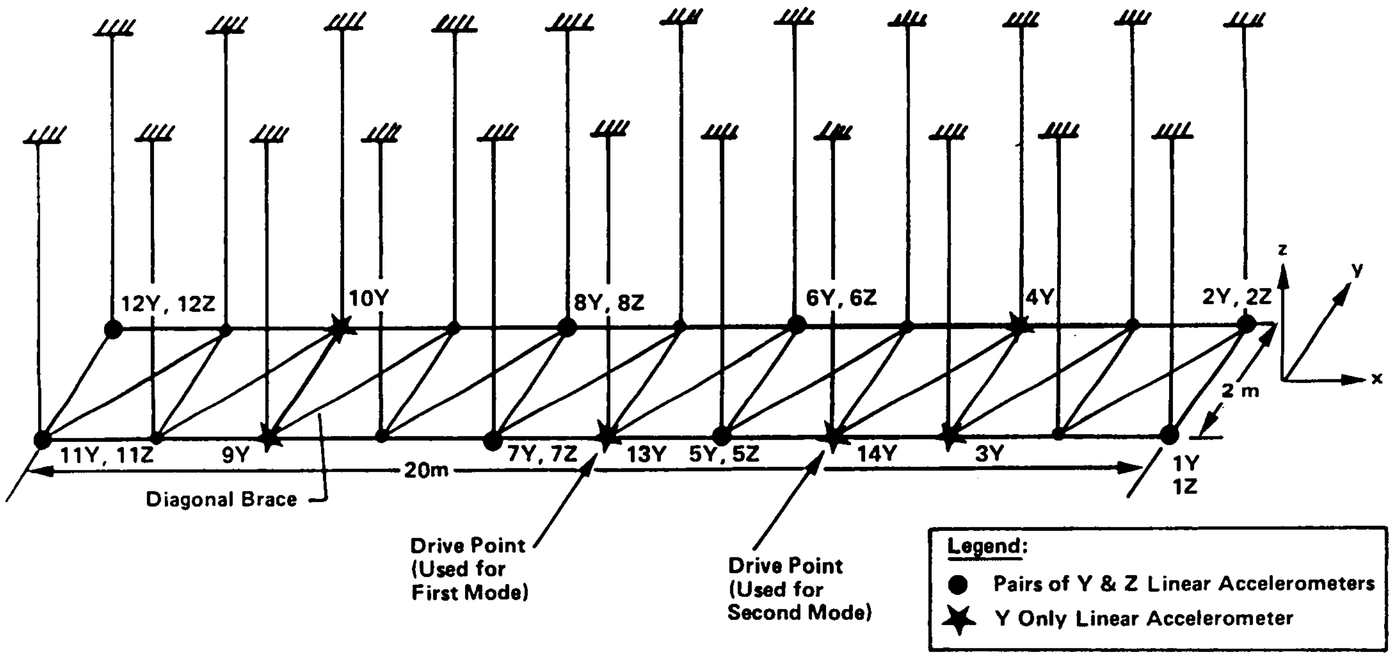

Figure 4 Schematic of Finite Element Model of Dynamic Truss

1) The rod elements representing the suspension system were not perpendicular to the truss plane.

2) The node points representing the corner fitting locations were out of plane by $\pm$ 0.02 inch.

Because previous analyses of large box truss space structures showed that pinned boundary conditions on the individual elements of a finite element model (FEM) were sufficient to represent the modal characteristics of the structure in the low frequency band, the test structure was modeled with beam elements pinned about the Z axis. (See Figure 4.) The beam elements were fixed (not pinned) about the Y axis, because element bending and axial elongation of the suspension wires provided the only stiffness in the X, Z plane.

Figure 5 shows the first four mode shapes and frequencies of vibration in the X, Y plane. (See Figure 4 for coordinates.) This type of motion will be referred to as in-plane motion. Analytical simulation of the imperfections noted above had very little influence on these modal characteristics. As indicated in Figure 5, these four in-plane modes are modes 26, 61, 72 and 83, a small subset of a large set of modes. The modes that are not shown are either low frequency, rigid truss, suspension system modes or out-of-plane modes.

To evaluate the out-of-plane response due to in-plane excitation, the frequency response of all modes of the structure, up to 80 Hz, was calculated (2% damping was assumed). Figure 6 shows typical in-plane (Figure 6-a) and out-of-plane (Figure 6-b) responses at node 2 due to excitation in the Y direction at node 13. (See Figure 4 for node numbers.) Out-of-plane response was predicted to be generally three orders of magnitude lower than in-plane response. The modes were recalculated, modeling beams as fixed ends (no pins), and the same frequency responses were generated. Similar ratios of in- and out-of-plane amplitudes were obtained. Note that only mode 26, at 19.9 Hz; mode 61, at 44.4 Hz; and mode 72 at 71.1 Hz were predicted to contribute to in-plane response.

In addition to verifying the suspension system design, the modal analysis was used to determine placement of the accelerometers and drive points on the truss. Figure 4 shows the locations of each accelerometer. A total of 22 linear accelerometers, 14 in-plane and 8 out-of-plane, were used. Fabrication of the test article under D-54D funding proceeded on the basis of this analysis.

The final D-54D effort on the box truss test structure was the random vibration test to measure the actual response of the structure and verify the prediction of small coupling between the X, Y, and XZ planes. Table 2 shows the results of that test.

Figure 5 Analytical Mode Shapes and Frequencies
Tube Diagonals, No Freeplay, All Pinned Joints
(All Axial Strain Energy)

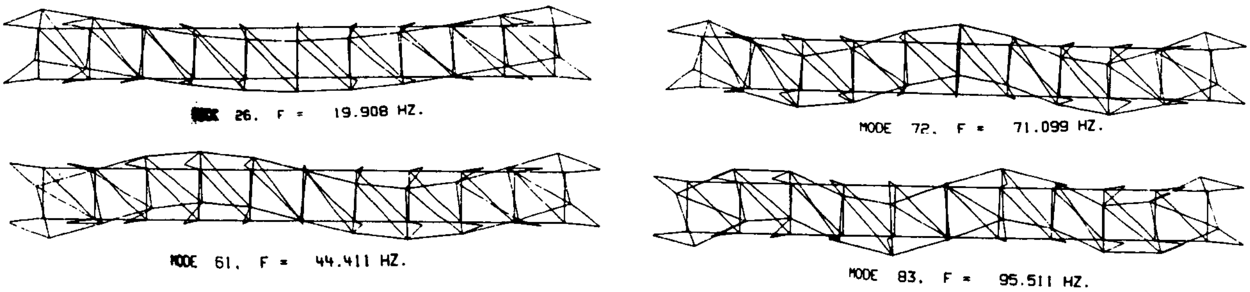

Figure 6 Frequency Response to in-Plane Force at Mid Span (F_{13Y})
(Pinned End Model)

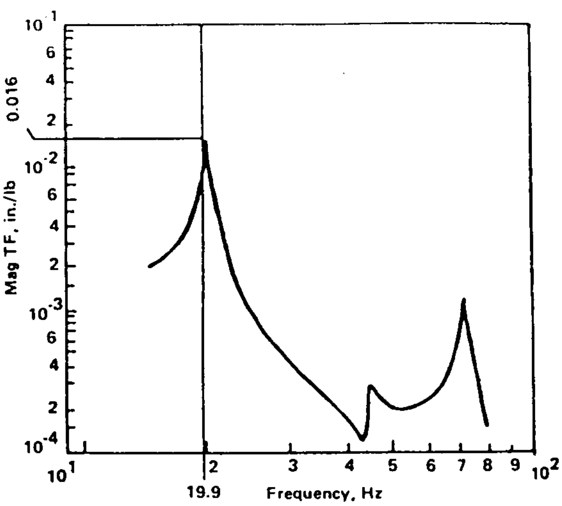

a) In-Plane Response
(Y_2/F_{13Y})

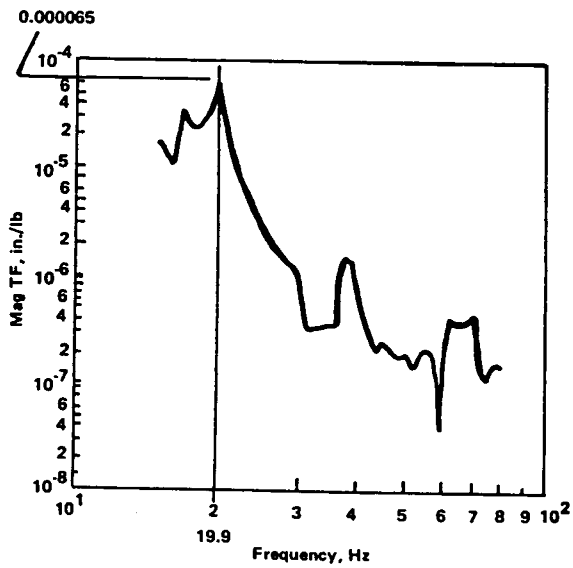

b) Out-of-Plane Response
(Z_2/F_{13Y})

Table 2 Transfer Function Magnitudes at 19.9 Hz

In-Plane		Out-Of-Plane	
Accelerometer	Magnitude in./lb	Accelerometer	Magnitude in./lb
1Y	0.066	1Z	0.0002
2Y	0.072	2Z	0.0006
3Y	0.005	--	--
4Y	0.005	--	--
5Y	0.043	5Z	0.004
6Y	0.043	6Z	0.004
7Y	0.044	7Z	0.002
8Y	0.045	8Z	0.002
9Y	0.004	--	--
10Y	0.006	--	--
11Y	0.062	11Z	0.004
12Y	0.067	12Z	0.000
13Y (Drive Point)	0.046	--	--

NOTE: Accelerometer locations are shown in Figure 4

4.0 DISCUSSION OF THE ANALYTICAL MODELS

As part of the effort under contract, the tube diagonal truss structure was weighed, the finite element model (FEM) was corrected to reflect this weight, and the modal characteristics were recalculated. (Accelerometers and attachment block weights were included in this model.) Again, two models were generated. One represented the ends of all elements as pinned joints. The other represented the ends of all elements as fixed joints (no pins). The FEM input data for this model is in Appendix A. This covered the full range of possible end conditions but did not cover intermediate conditions, some joints fixed, some pinned. The pinned-end model results already have been shown in Figure 5. The fixed-end model (no pins) results are shown in Figure 7. As noted in the discussion of the pinned-end model results, only that subset of in-plane modes are presented. The obvious difference between pinned- and fixed-end model results is the great increase in the number of in-plane modes resulting from fixing the elements at the joints. This condition was first observed on this test article when comparison of test results with analytical predictions began. The reason for this difference in fixed- vs. pinned-end modes is discussed here to avoid disrupting continuity of the discussion of test results that will follow.

The first step in understanding the fixed-end modes is to observe that there appear to be several first and second beam bending type modes. Because mode shapes are unique, all but one first and second mode shape must represent some other type of motion. It was determined that the other type of motion consists of local bending of the elements of the truss. This is not observable in the mode shape plots, because only translation displacements are plotted, and the model has degrees of freedom (DOF) only at the joints of the structure. A review of the printout of modal amplitudes for the fixed ends model shows relatively large rotations at joints in those modes that represent primarily local bending. An alternative way to identify the type of mode is to calculate and review the percentage of axial, torsional, and bending (about Y and Z axes in Figure 4) strain energy in each element of each mode. The details of this method were first developed under Martin Marietta Denver Aerospace IR&D project D-28R and published as "Eigensolution Sensitivity to Parametric Model Pertubations" in the Shock and Vibration Bulletin No. 46, Part 5, August 1976. Later, this strain energy method was applied, again under Martin Marietta's project D-28R, to develop "Design Criteria to Assure Pinned-End Truss Behavior Below Selected Frequency", published as IR&D report R84-48628-001, November 26, 1985. This strain energy method can be summarized as follows:

Figure 7 Analytical Mode Shapes, Frequencies, and Strain Energy
Tube Diagonals, No Freeplay, Fixed Ends (No Pinning)

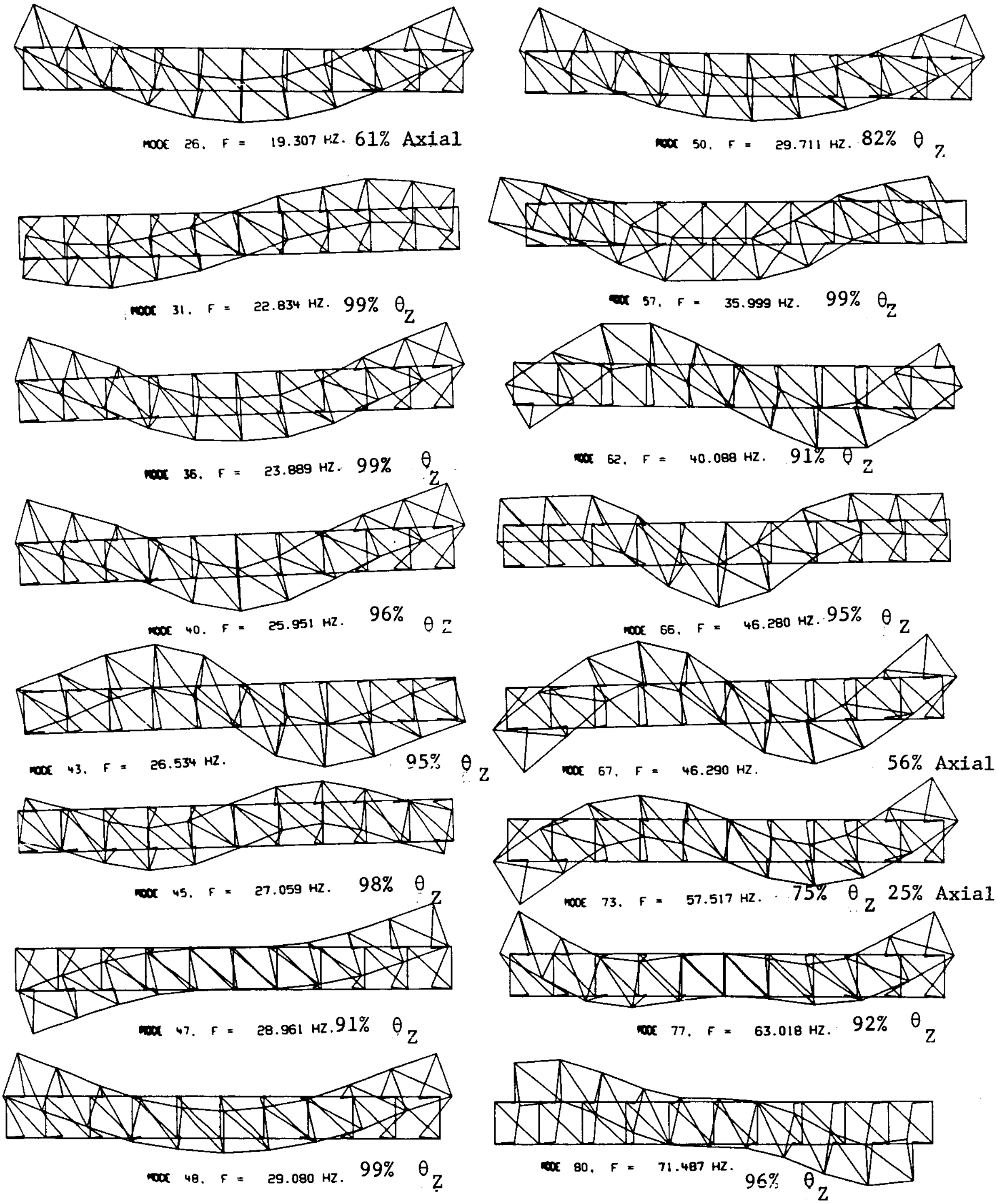

- Total strain energy, SE, per unit defection of the ith modal coordinate is

$$SE_i \equiv \omega_i^2 = \sum_{j=1}^{NE} \phi_i^T K_j \phi_i$$

  Note that the strain energy in any element can be further subdivided to indicate direction of strain, e.g. beam strain energy can be subdivided into axial, torsional and bending components.

- The influence that any jth element, or subset of elements, has on determining the frequency of a given mode is proportional to the fractional part of strain energy contained in that element or subset of elements.

- Therefore, if a beam element of a truss FEM, modeled with fixed ends, contains only axial strain energy in a mode, the rotational fixity conditions at joints are not important. That mode will appear as the same mode shape and frequency with either fixed- or pinned-end joints. This is the case for first global mode of the box truss being tested as seen by comparing mode 26 in Figure 5 with mode 26 of Figure 7.

- Conversely, if a beam element of a truss FEM, modelled with fixed ends, contains primarily bending strain energy in a mode, the rotational fixity conditions at joints determine the frequency of the mode and element bending is the primary type of modal motion. Consequently, if that same model is revised to represent pinned-end elements, no element bending modes will be predicted. This case also is exhibited by the test article as is evident by many element bending modes predicted by the fixed-end model in Figure 7 and not predicted by the pinned-end model of Figure 5.

The bending frequencies of the 2-meter truss elements (see Section 3 for dimensions) with pinned-pinned and free-free end conditions were calculated to be 19.9 Hz and 45.2 Hz, respectively. The behavior of any element, when oscillating in a global mode, should reflect boundary conditions somewhere in this frequency range. Although the analysis (Figure 7) does not consider such nonlinearities as variations of boundary conditions and oscillating end load effects on element bending frequencies, the beginning of in-plane coupling effects first become evident at 22.834 Hz (mode 31).

So far, this section has discussed only the tube diagonal configuration. An analysis of the tension diagonal configuration was also performed. The FEM was modified by replacing the single aluminum tube diagonals with two steel rod diagonals having a fitting mass at the diagonal intersection point. The combined stiffness of two steel rods was intended to be equal to the stiffness of a single aluminum tube, so that in-plane behavior of the tension diagonal configuration would be the same as that of the tube diagonal configuration. However, stock 3/16-inch steel rod was used for economy and the measured weight of the truss was 6.6 lbs heavier than the aluminum diagonal configuration. As a result, the first and second global bending frequencies of tension diagonal configuration were 17.3 Hz and 53.48 Hz, respectively. The FEM input data for this model is in Appendix B. Out-of-plane modes are different because of the additional nodes at the rod intersections. Because only in-plane motion is relevant for test correlation, the analytical mode shape data of Figure 7 is applicable for both the tube and tension diagonal configurations.

The strain energy distribution was not calculated for the pinned-end model because all energy must be axial with pinned ends. The strain energy distribution was calculated for the fixed-end model, and the results are summarized as the percentage (%) values shown in Figure 7. Note that most modes shown are strongly in-plane element bending modes (See θ_Z direction in Figure 4.) Those modes not included in Figure 7 are strongly θ_Y bending (or axial suspension) strain energy modes.

5.0 TEST SETUP AND DATA REDUCTION

The test setup was the same as that described in discussion of the IR&D progress in Section 3. After weighing the structure, the test configuration was reestablished on the suspension system, and theodolites were used to assure a planar truss within $\pm$ 0.02 inches tolerance.

All accelerometers were PCB models of Type 380B02. Figure 4 identified their locations and directions. The modal survey was conducted using single-point random excitation. During all tests, state-of-the-art equipment was used to record the response. When the response in the time domain was recorded, a magnetic tape recorder, Honeywell 101 Electronics; a Gould waveform recorder, amplifier Model 13-4616-10; and a millimeter, Fluke 8810 Voltmeter were used. Some of the time history data were then plotted on paper using a Gould strip chart 8-channel recorder Model 2800.

The time histories were then fed to a HP545K computer system where fast Fourier transform calculations generated the real and imaginary components of the complex transfer functions, acceleration/input force, for each measurement. State-of-the-art curve fit of these transfer functions were calculated to identify the parameters of mode shapes, frequencies and modal damping.

6.0 TEST RESULTS

6.1 Test Results for Box Truss with Tube Diagonals, No Freeplay

Figure 8 shows the absolute magnitude of some typical frequency response functions for the box truss with tube diagonals and no freeplay, forced in the Y direction at node 13. All scales are linear. The abscissae of these plots show the frequency from 0 to 50 Hz. The ordinate scales are normalized to the maximum value of the magnitude of the transfer function. The letter m following a number denotes 10^{-3}.

Identification of a particular transfer function is given at the top of each plot, e.g., -2Y/-13Y indicates accelerometer 2 in the Y direction/force at node 13 in the Y direction. These and other similar transfer functions identify two modes, one at 20 Hz and one at 40.61 Hz. Figure 9 shows the corresponding test determined mode shapes. The first mode at 20 Hz correlates well with the analytically predicted first global bending mode (mode 26 of Figures 5 or 7). The 40.61 Hz test mode of Figure 9 does not correlate in frequency with any analytically predicted mode even though many of the predicted shapes that result from local element bending, as discussed in Section 4.0, do correlate to some extent. One can only speculate that frequency correlation is poor because end loading, due to global motion on elements that are bending locally, lowers the bending frequency both locally and globally. (For example, mode 66 of Figure 7 at 46.28 Hz might be shifted down to 40 Hz as a result of this phenomenon.) However, the amount of test data is insufficient to state this as a conclusion. In Section 6.5, many of these local bending type modes are identified. Further discussion on the validity of such data is presented in that Section.

Figure 10 shows the absolute magnitude of some typical frequency response functions for the box truss with tube diagonals and no freeplay, forced at node 14 in the Y direction. The abscissae of these plots show the frequency from 0 to 60 Hz, and a third mode at 55.84 Hz is evident from these plots. Figure 11 shows the corresponding test determined mode shape. The shape is that of a second free beam bending mode and correlates in shape with the second global in-plane mode 61 at 44.411 Hz of Figure 5, and with several modes shapes of Figure 7. Mode 67 of Figure 7 was expected to correlate with a global test mode, rather than any other, because mode 67, being 56% axial strain energy, is more closely related to the pinned-end result in Figure 5. The fixed-end analysis result of mode 67 at 46.29 Hz is of higher frequency than the pinned-end analysis result of 44.411 Hz, because the fixed-end analysis contains bending as well as axial strain energy. However, neither analytical frequency is as high as the test frequency of 55.84 Hz.

Figure 8 Test Transfer Functions (Absolute Magnitude) for Box Truss with Tube Diagonals and No Free Play, Shaker at Node 13, Y Motion

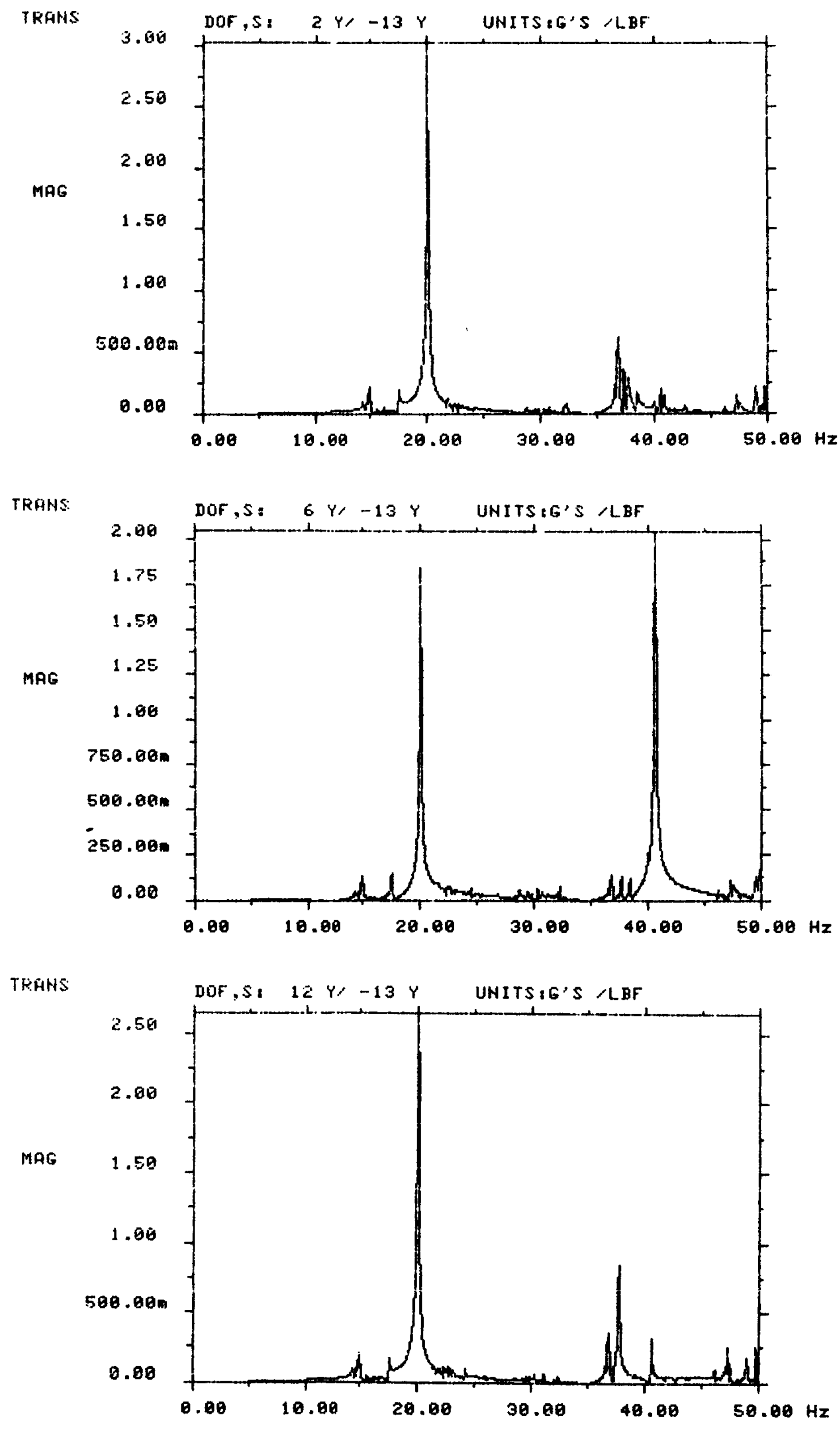

Figure 9 First and Second Measured Mode for Box Truss with Tube Diagonals and No Free Play

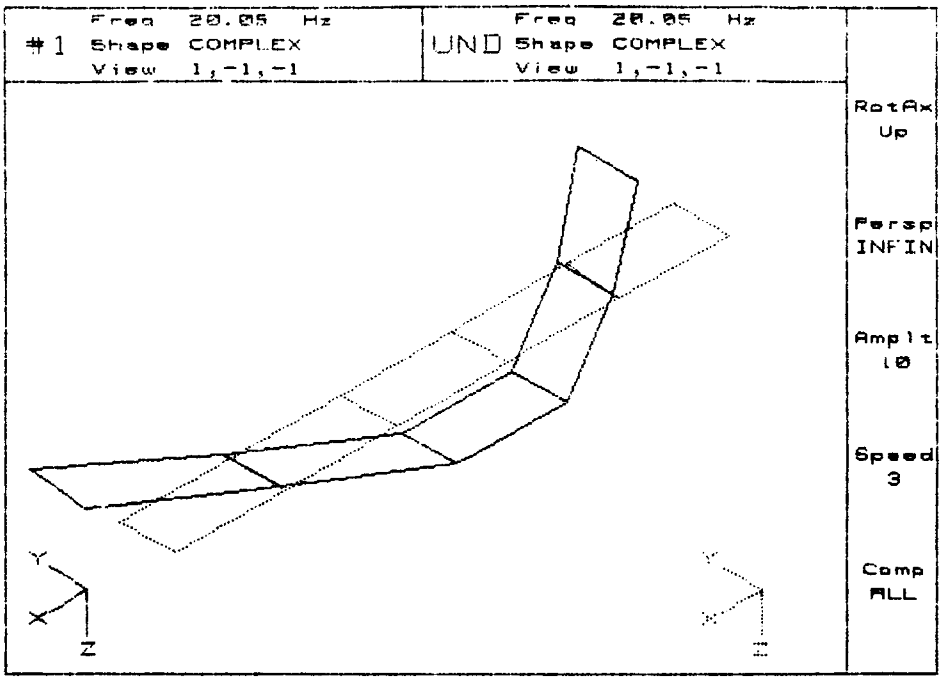

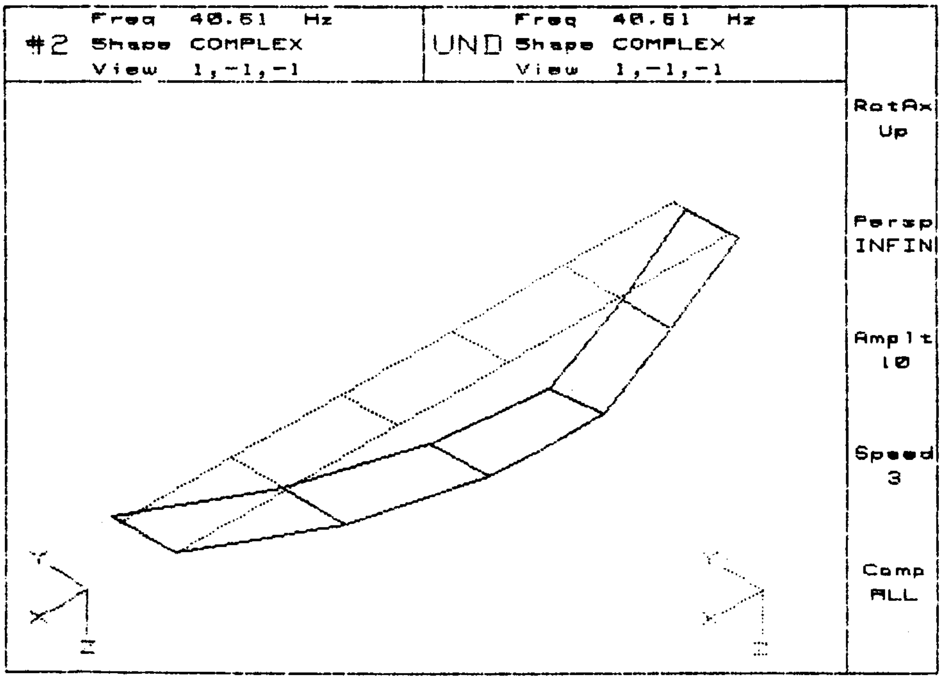

Figure 10 Test Transfer Functions (Absolute Magnitude) for Box Truss with Tube Diagonals and No Freeplay, Shaker at Node 14, Y Motion

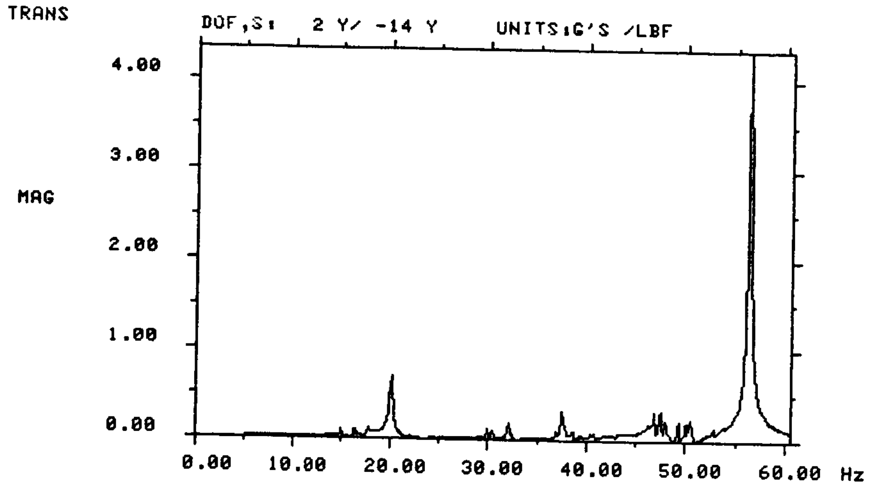

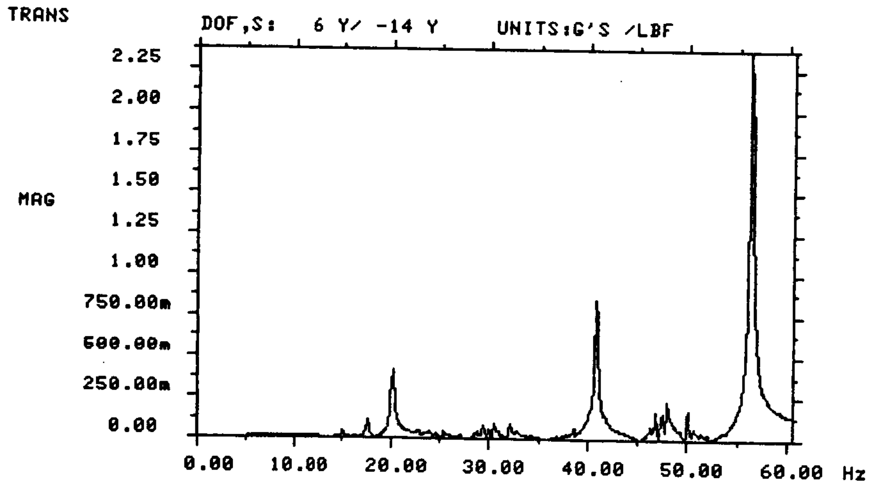

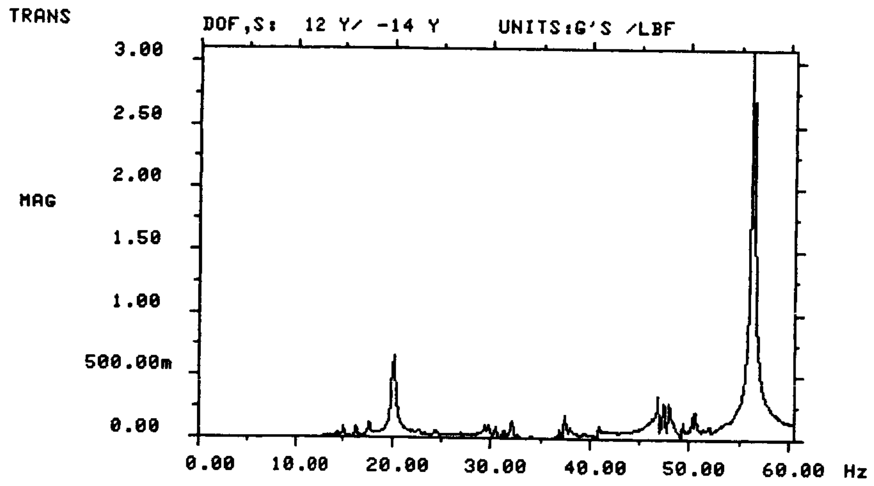

Figure 11   Third Measured Mode for Box Truss with Tube Diagonals and no Free Play

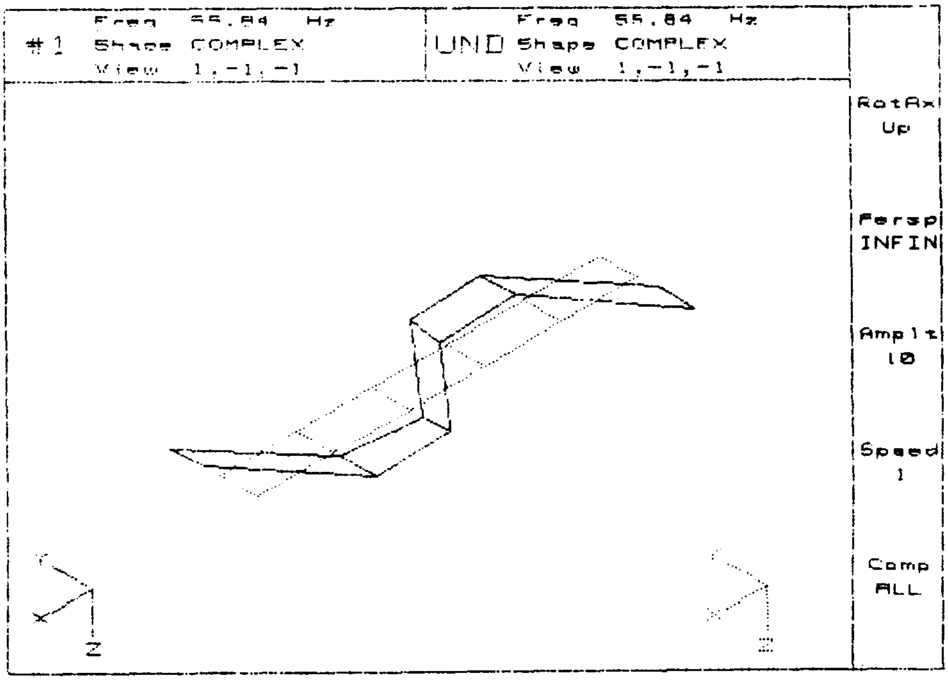

The next best alternative correlation for this 55.84 Hz test mode exists with analytical mode 73 at 57.517 Hz. The modal amplitude at the shaker (node 14) in mode 73 is 1.617. The modal amplitude at the shaker in mode 67 is 2.485 which is only 54% greater than in mode 73. Also, mode 73 is 25% axial strain energy. Therefore, it is not unreasonable to speculate that mode 73, or some combination of modes 67 and 73, was observed in the test.

A third effort to establish theoretical/experimental correlation was made. The analytical model was expected to be softer than for the real structure because beam elements were modeled from node to node with the same area, whereas joint structure and end fittings are much stiffer than the tubes because their area is much greater. An analytical estimate of this effect was made using the strain energy method cited in Section 4.0. This was done by estimating the increase in axial and bending stiffness due to the end fittings of the FEM members. Assuming the flexible length of tube is decreased by 6 inches on each end, the axial stiffness increases by

$$K_p^* = K_p \frac{78.74}{78.74-12} = K_p(1.18), \quad \text{i.e., an 18\% increase.}$$

The bending stiffness increases by

$$K_m^* = K_m \left(\frac{78.74}{78.74-12}\right)^3 = K_m(1.64), \quad \text{i.e., a 64\% increase.}$$

The axial strain energy in mode 67 is 56% (see Figure 7). The remaining strain energy, 44%, is in bending.

The strain energy method calculates the frequency shift due to these stiffness changes from

$$f_{67}^* = 46.29 \sqrt{1 + .18(.56) + .64(.44)} = 54.4 \text{ Hz}$$

which compares well with the measured 55.84 Hz. Similarly, an estimate of mode 73 frequency shift is

$$f_{73}^* = 57.517 \sqrt{1 + .64(.75) + .18(.25)} = 71.03 \text{ Hz}$$

which is out of the frequency range of the observed response. Future testing to measure these and other local joint and end-fitting properties has been proposed.

Linearity of the tube diagonal truss configuration without freeplay was checked in two ways. First, the structure was excited sinusoidally at each of the modal frequencies identified above by the single-point random excitation. At each frequency, the excitation force was increased by a factor of 10, and no non-linear behavior was observed. Second, the transfer function obtained from measuring in-plane response at node 14 while forcing in-plane at node 13 was compared to that measured at node 13 while forcing at node 14. The result, shown in Figure 12, indicates symmetry, thereby fulfilling Maxwell's Reciprocity requirement for a linear structure. Note, that these results are the absolute value of the magnitude of the transfer function expressed in decibel units (i.e., dB = 20 log (G/lb).

Figure 12 Measured Transfer Functions in Y Direction at Node 13 and 14

(Y_{14}/F_{13} and Y_{13}/F_{14})

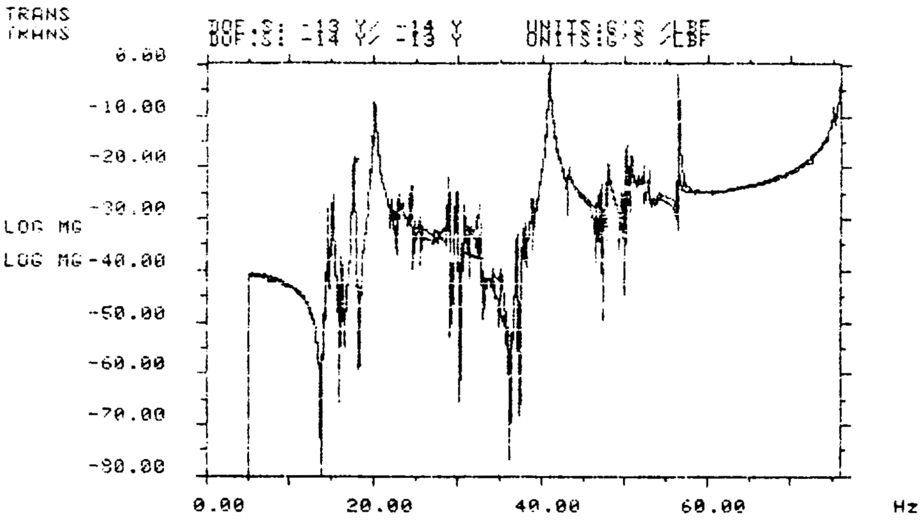

6.2 Test Results for Box Truss with Tube Diagonals and 3 mil Joint Freeplay

The second test was performed on the box truss with tube diagonals and 3 mil freeplay at each joint. No modal analysis could be performed on this non-linear configurations. Figure 13 presents typical test transfer functions for the box truss with tube diagonals and 3 mil freeplay. These plots correspond to those for the no freeplay case previously given in Figure 8.

Note the amplitude of the 3 mil freeplay peaks are one to two orders of magnitude less than the no freeplay results.

Although peaks suggest the existence of a mode around 25 Hz, curve fitting of the data did not identify any modal characteristics. An unsuccessful attempt was made to excite the structure sinusoidally at the frequencies of the modes that were identified by testing the no-freeplay configuration described in Section 6.1. Time histories from these sinusoidal tests (not shown) reveal large nonlinearities. This is why no modal characteristics could be detected by the nominal curve fit process which is based on the assumption of linearity.

6.3 Test Results for Box Truss with Tube Diagonals and 1 mil Joint Freeplay

The third test was performed on the box truss with tube diagonals and 1 mil freeplay at each joint. No modal analysis could be performed on this non-linear configuration. Figure 14 presents typical in-plane test transfer function for this configuration driven at node 13. These plots correspond to those for the no-freeplay case previously given in Figure 8.

Figure 14 indicates two obvious modes around 18 Hz and 32 Hz. Figure 15 shows four modes identified by curve fitting the transfer functions of Figure 14. The amplitudes at which the mode shapes are displayed in Figure 15 are arbitrarily set by the computer operator, tending to imply equal importance to each mode shown. Actually, each of the modes, except the second at 17.72 Hz has considerable out-of-plane motion. This is evident in the corresponding Z motion transfer functions shown in Figure 16. This Z motion is of the same magnitude as Y motion (Figure 14) except in the region of 17.4 Hz. The large Z motion in the 12.15 Hz mode suggests this is more likely an out-of-plane than an in-plane mode. Consequently, only the second mode correlates directly with mode 26 (Figure 7) at 19.307 Hz. The other modes in Figure 15 may be manifestations of other in-plane analytical predictions in Figure 7 but local distortions, as displayed by the fourth mode in Figure 15, make certain correlation impossible. The difference in frequency between the 19.307 Hz analytical mode and the 17.72 Hz test mode is consistent with the shift predicted by the "Modal Freeplay Method" developed by Martin Marietta. The following discussion explains this method.

We assess the effect of freeplay on a mode in a manner similar to that of Timoshenko*.

* S. Timoshenko: "Vibration Problems in Engineering." B. Van Nostrand Inc., New York, NY, 1956.

Figure 13 Test Transfer Functions (Absolute Magnitude) for Box Truss with Tube Diagonals and 3 mil Freeplay Shaker at Node 13

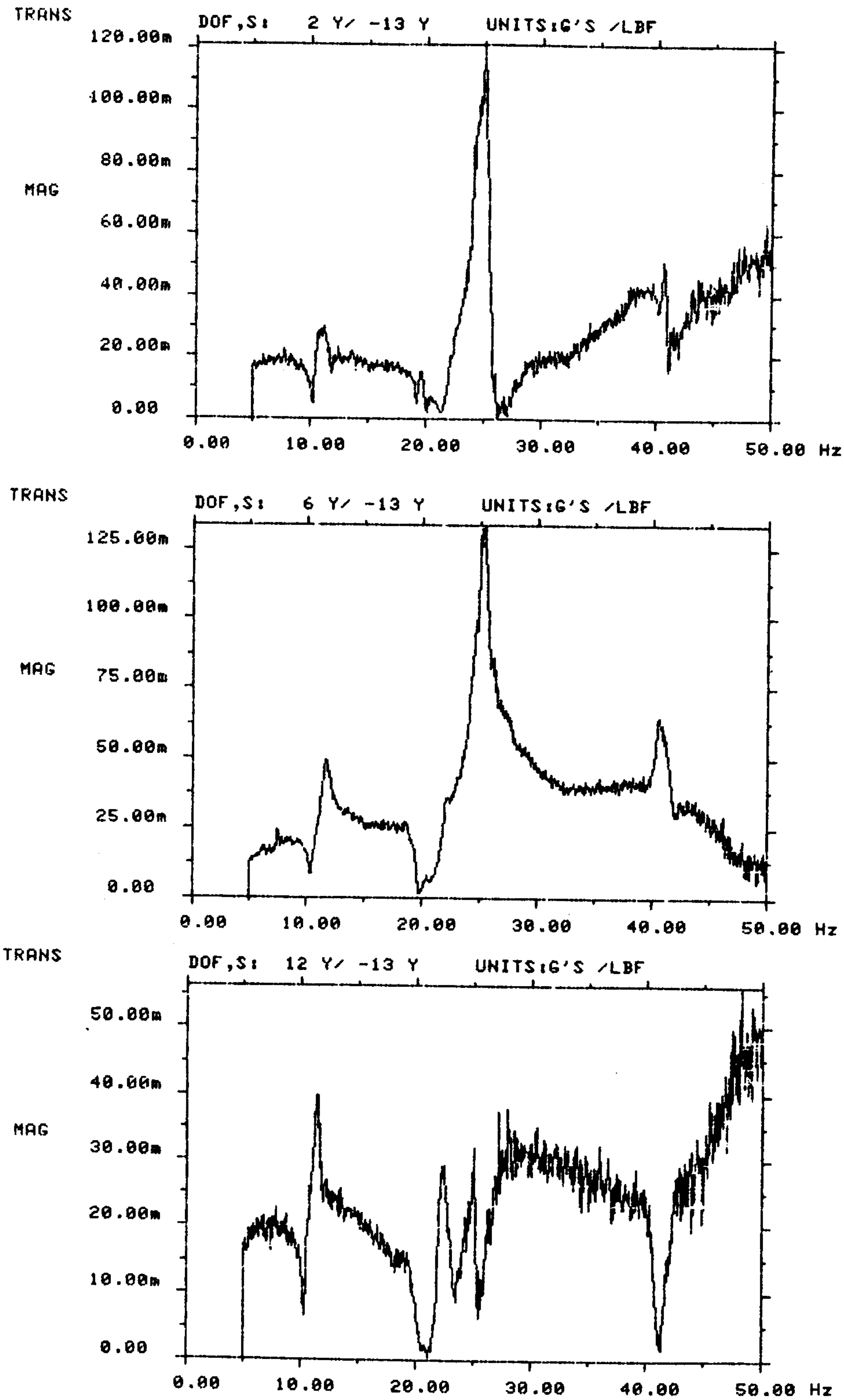

Figure 14 Test Transfer Functions (Absolute Magnitude) for Box Truss with Tube Diagonals and 1 mil Freeplay, Shaker at Node 13, Y Motion

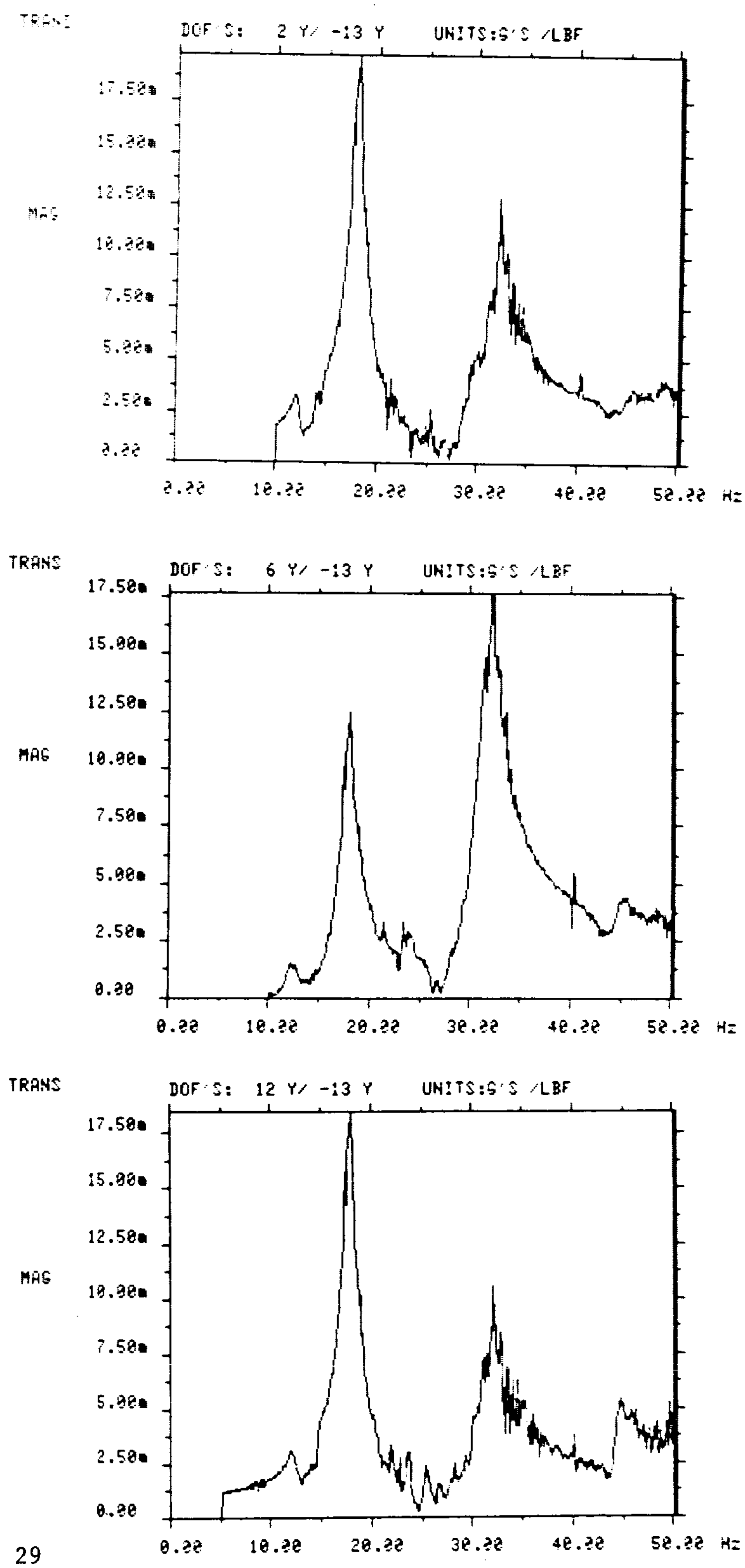

Figure 15 Measured Modes for Box Truss with Tube Diagonals and 1 mil Freeplay, Shaker at Node 13, Y Motion

MODAL FREQUENCY & DAMPING

MODE NO	FREQUENCY (HZ)	FREQUENCY (RAD/SEC)	DAMPING (HZ)	DAMPING (RAD/SEC)	DAMPING (%)
1	12.145	76.312	0.422	2.654	3.476
2	17.724	111.363	0.644	4.046	3.631
3	31.426	197.458	0.800	5.029	2.546
4	44.725	281.014	0.417	2.617	0.931

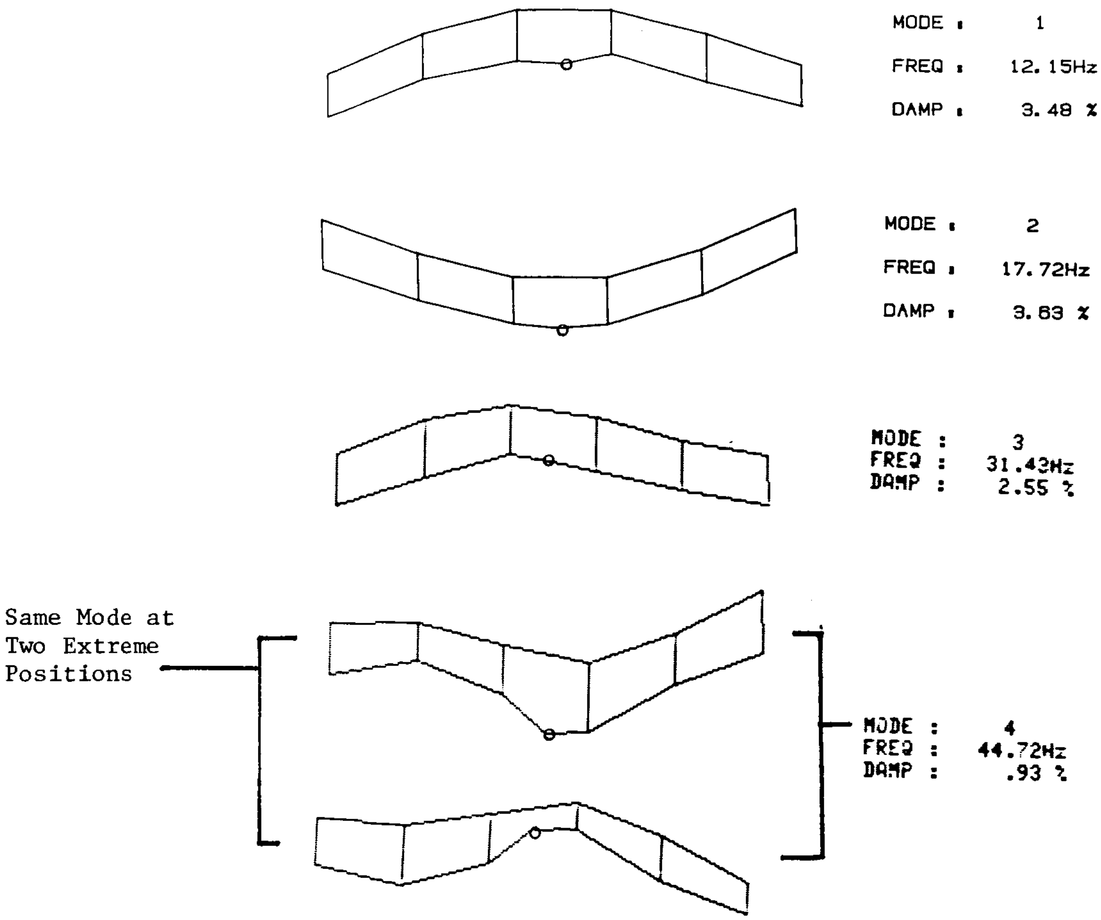

o Shaker Location

Figure 16 Test Transfer Functions (Absolute Magnitude) for Box Truss with Tube Diagonals and 1 mil Freeplay, Shaker at Node 13, Z Motion

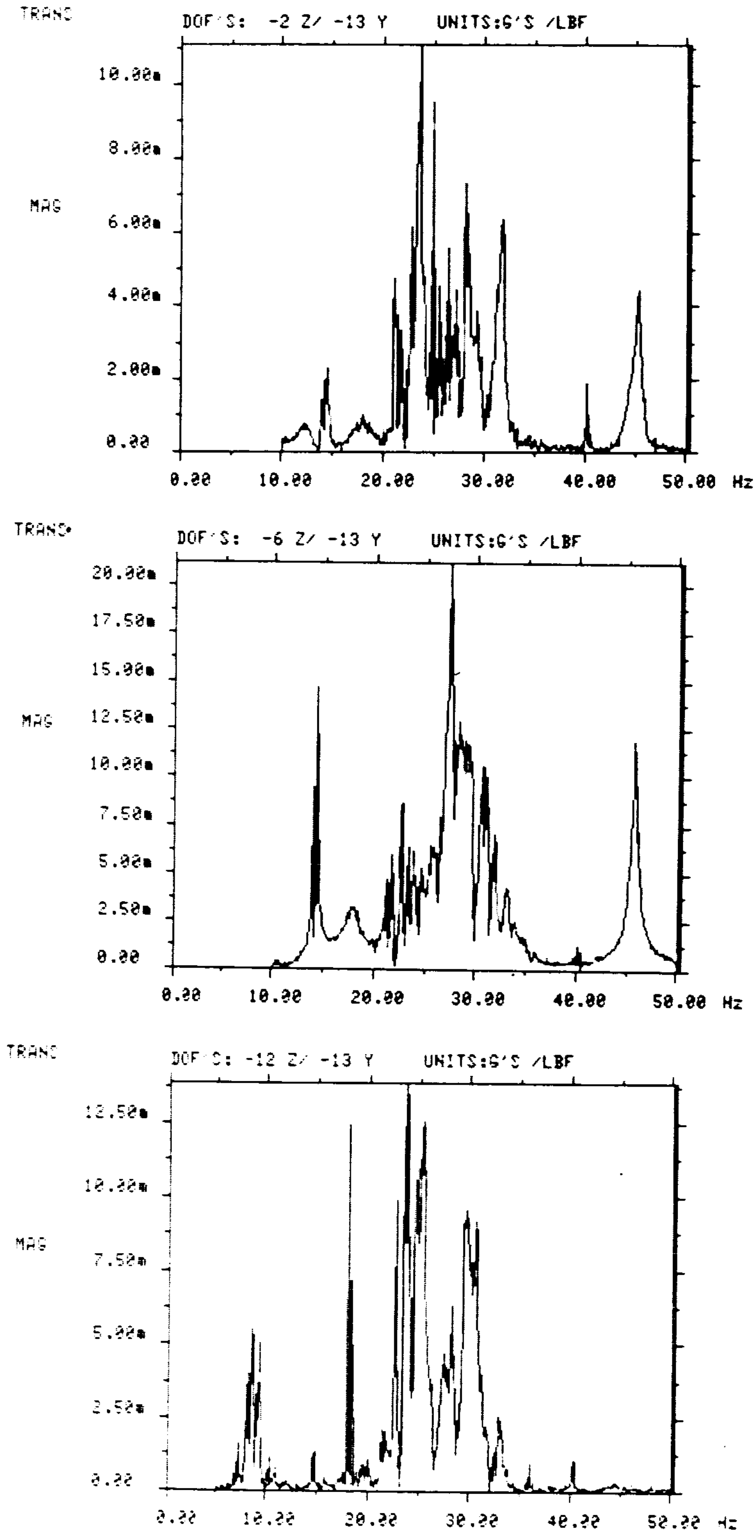

The approach is an extension of the single-degree-of-freedom analysis of the nonlinear system (Figure 17.a.1). A mass, m, performs vibrations between two springs by sliding without friction along the bar, AB. Measuring the displacements from the middle position of the mass, m, the variation of the restoring force with the displacement can be represented as shown in Figure 17.a.2. The frequency of the vibrations will not only depend on the spring constant, but also on the magnitude of the clearance, a, and on the initial conditions. Assume, for instance, that at the initial moment (t = 0) the mass, m, is in its middle position and has an initial velocity, v, in the x-direction. Then, the time necessary to cross the clearance, a, will be

$$t_1 = a/v.$$

After crossing the clearance, the mass, m, comes in contact with the spring and further motion in the x-direction will be simple harmonic.

The time during which the velocity of the mass is changing from v to 0 (quarter period of the simple harmonic motion) will be

$$t_2 = \frac{2\pi}{4}\sqrt{\frac{m}{k}}$$

where k is the spring constant for one spring. The complete period of vibration of the mass, m, is

$$\tau = 4(t_1 + t_2) = 4a/v + 2\pi\sqrt{\frac{m}{k}}$$

For a given magnitude of clearance, a given mass, m, and a given spring constant, k, the period of vibration depends only on the initial velocity, v. The period becomes very large for small values of v and decreases with increase of v, approaching the limit $\tau_0 = 2\pi\sqrt{m/k}$ (Fig. 17.a.2) when $v = \infty$.

Such conditions are always obtained if there are clearances in the system between the vibrating mass and the spring.

If the clearances are very small, the period, τ, remains practically constant for the larger part of the range of the speed, v, as shown in Figure 17.a.3 by curve I. With an increase in clearance for a considerable part of the range of speed, v, a pronounced variation in period of vibration takes place (curve II, Figure 17.a.3). The period of vibration of such a system may have any value between $\tau = \infty$ and $\tau = \tau_0$.

1) 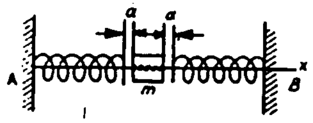

Single-Degree-of-Freedom Freeplay Model

2) 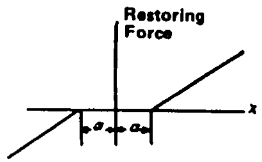

Nonlinear Force versus Displacement

3) 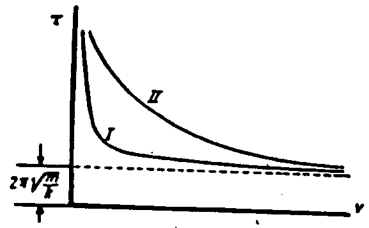

Period versus Velocity

0 PERIOD WHEN a = 0

$$\tau_1 = 2\pi\sqrt{\frac{m}{k}}$$

0 TIME PER CYCLE PASSING THROUGH a

$$\tau_2 = 4\frac{a}{\dot{V}}$$

WHERE $\dot{V}$ DEPENDS ON AMPLITUDE OF VIBRATION

0 PERIOD WHEN a $\neq$ 0

$$\tau = \tau_1 + \tau_2$$

Figure 17.a Modal Freeplay Development

Figure 17.b represents the circular arc shape that would be taken if all elements were of identical length and all hole diameters were 0.001-inch larger than the diameter of the pins at every joint. This figure also shows the shape of the fundamental elastic mode of the same truss for no freeplay conditions. Under the assumption that the mode shape will be little affected by passage through the freeplay region, an estimate of the "modal freeplay" amplitude, δ, can be obtained by locating the nodes of the elastic mode shape in the corresponding location of the circular arc of Figure 17.b. This modal freeplay is equivalent to the gap, a, in Figure 17.a.1. The velocity at the center of the beam can be expressed in terms of modal parameters and a sinusoidal force applied at some point on the truss. At steady-state conditions, the velocity is

$$v = \frac{\phi(X=\frac{L}{2})\ \phi(X=0)}{2\zeta\ M_{eq}\ \omega}\ F_o$$

Substituting this velocity, the modal freeplay, and the linear model modal frequency into the period equation, the variation of first mode period with amplitude of the applied force was calculated. Figure 17.c shows the results for 1 mil of joint freeplay ($\zeta = 0.01$ was assumed).

As the applied force increases, the freeplay period of oscillation approaches that of the system without freeplay. The test was conducted with random excitation having a 0.5 lb to 1 lb RMS force from 5 Hz to 80 Hz. Therefore, the test frequency of 17.72 Hz corresponds to a period of 0.0564 sec which is well in the range of the values predicted by the modal freeplay method at the low force level in Figure 17.c.

Figure 18 presents typical in-plane transfer functions for this configuration driven at node 14. Modes around 18 Hz, 32 Hz, 43 Hz and 52 Hz are indicated by the peak of the transfer functions. Figure 19 lists the modal frequencies identified by curve fitting the transfer functions. Note that, except for the 51.587 Hz, these frequencies are close to those identified in Figure 15 from excitation at node 13. Because of the uncertain quality of modes 1 through 3, resulting from out-of-plane coupling, only the 51.59 Hz mode is shown. This is the second global bending mode of the tube diagonal truss with 1 mil freeplay which corresponds to the 55.84 Hz mode in Figure 11 measured without freeplay.

The decrease in frequency is consistent with the increase in freeplay, but no attempt has been made to predict this second mode frequency shift by the modal freeplay method. Exact correlation of this mode with analytical predictions is difficult for the same reasons as stated for the 55.84 Hz test mode in Section 6.1 plus the difficulty introduced here by the freeplay. However, it is still reasonable to speculate that the 51.59 Hz test mode in Figure 19 is some form or combination of modes 67 at 46.29 Hz and 73 at 57.517 Hz in Figure 7.

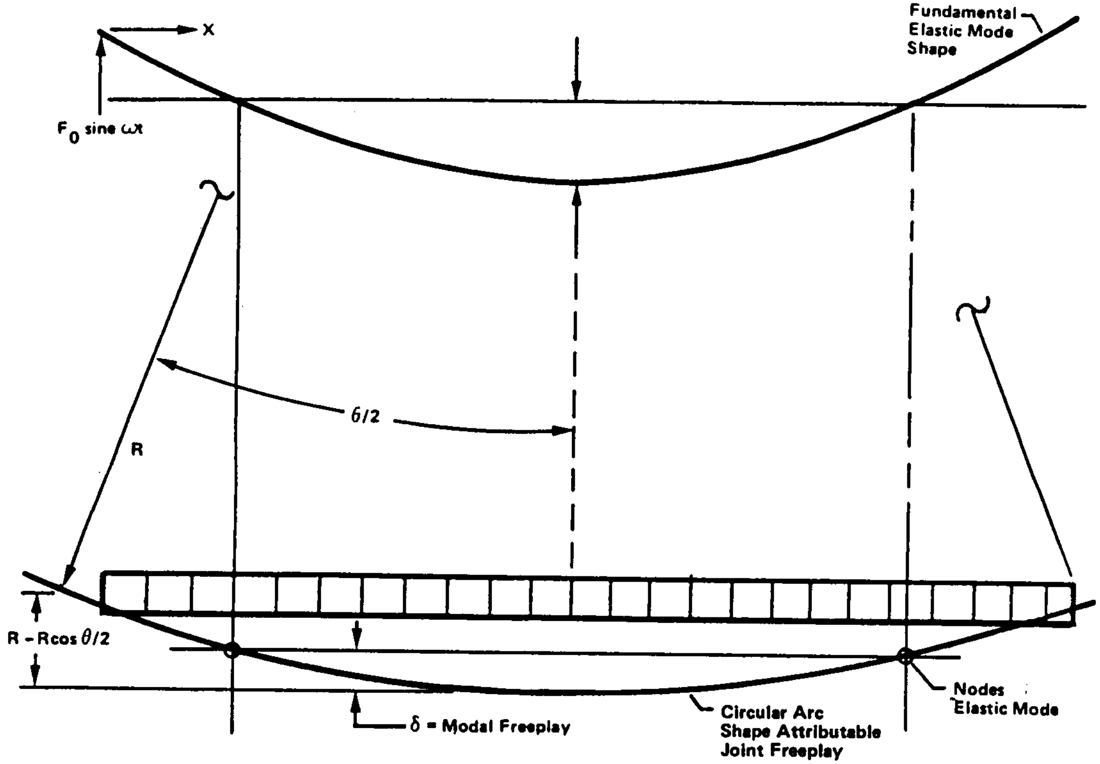

Figure 17.b Modal Freeplay Assessment Model

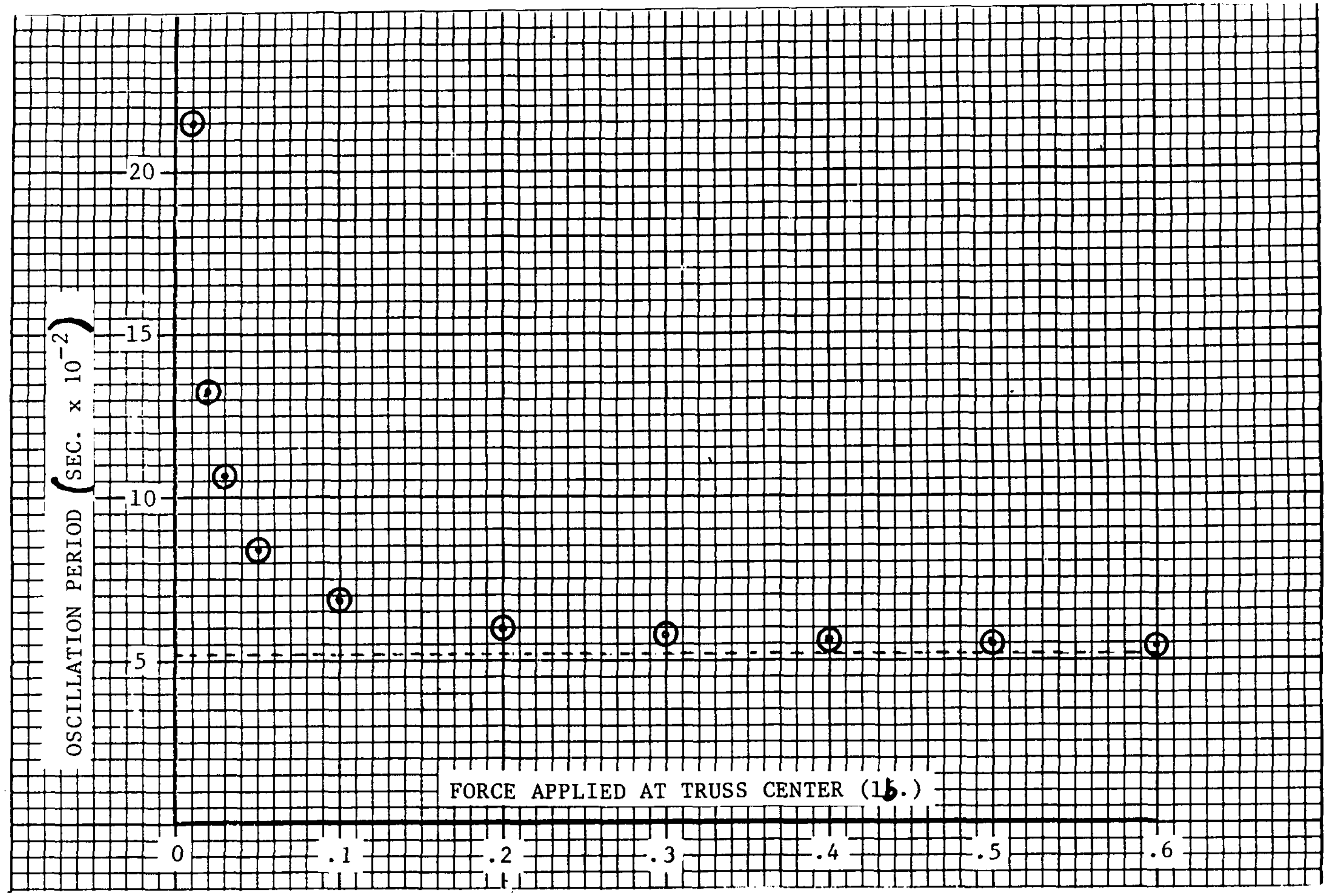

Figure 17.c Modal Freeplay Results, Period vs. Force, for Tube Diagonals, 1 mil Freeplay, Force Node 13

Figure 18 Test Transfer Functions (Absolute Magnitude) for Box Truss with Tube Diagonals and 1 mil Freeplay, Shaker at Node 14, Y Motion

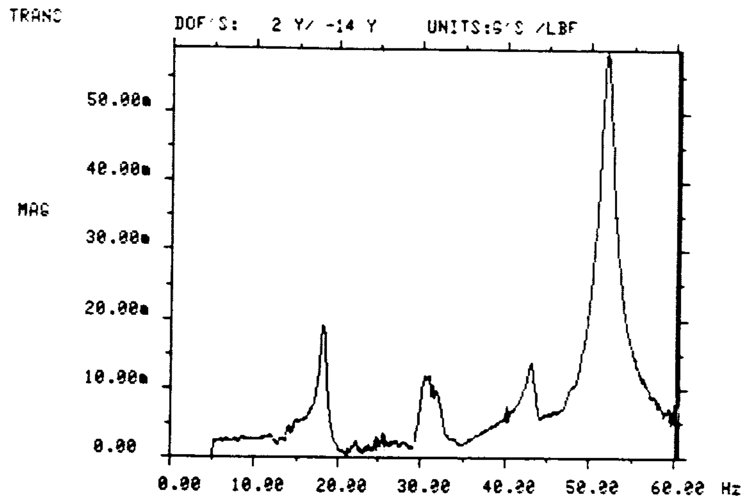

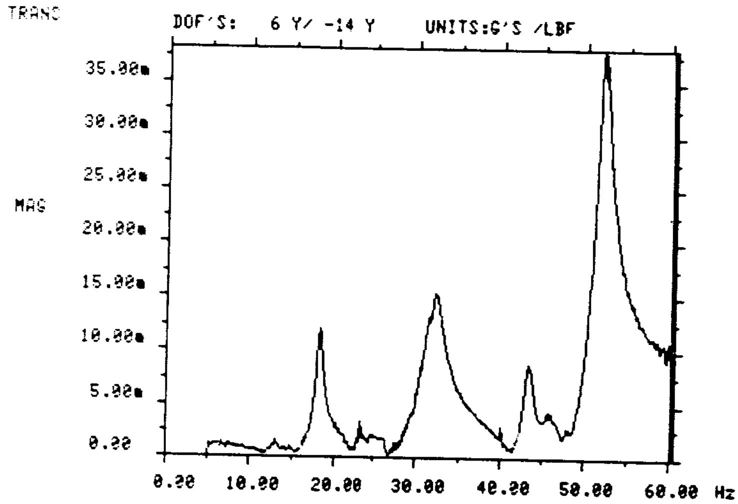

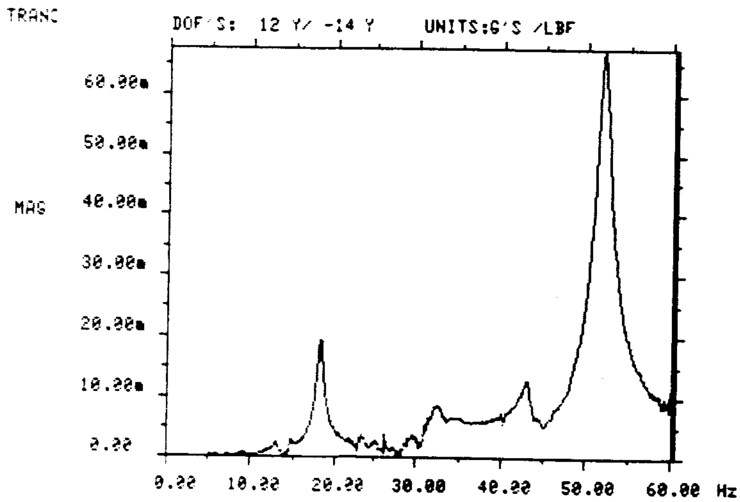

Figure 19 Measured Modes for Box Truss with Tube Diagonals and 1 mil Freeplay, Shaker at Node 14, Y Motion

MODAL FREQUENCY & DAMPING

MODE NO	FREQUENCY (HZ)	FREQUENCY (RAD/SEC)	DAMPING (HZ)	DAMPING (RAD/SEC)	DAMPING (%)
1	18.029	113.277	0.369	2.319	2.047
2	31.389	197.223	0.940	5.903	2.992
3	42.987	270.097	0.521	3.274	1.212
4	51.587	324.132	0.846	5.314	1.639

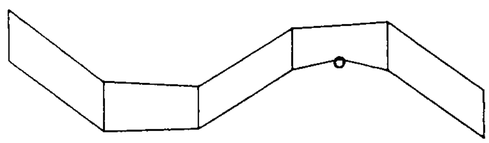

MODE : 4

FREQ : 51.59Hz

DAMP : 1.64 %

o Shaker Location

6.4 Test Results for Box Truss with Tension Diagonals and No Joint Freeplay

Results discussed in this section are from the first test of the box truss with the single aluminum tube diagonal replaced by two steel rod diagonals. These diagonals were pretensioned to 40 lbs. The terminology, freeplay, is a misnomer for the tension diagonal configurations, because the tension diagonals remove freeplay by making the joint pins bear against the holes. The more accurate description of the two tension diagonal configurations is clamped and unclamped. The unclamped configuration is established by installing the steel rod diagonals, with center intersection fittings, inserting bolts 1 mil smaller than the holes at all joints, and then using turnbuckles to establish the rod tension while monitoring calibrated strain gauges on the rods. The clamped configuration is established by inserting shims between the end fittings and the truss members so that a moment can be transmitted by the joint when the bolts are tightened. With the low level of random excitation (0.5 to 1 lb RMS from 5 to 80 Hz), response amplitudes were not large enought to relieve truss member preloads. (Minimum preloads in the X oriented members shown in Figure 4 were 40 lb (Cos 45°) = 28.3 lbs.)

This section presents test results of the clamped configuration. Figures 20 and 21 present the respective test transfer functions and modal characteristics obtained for the clamped (no freeplay) tension diagonal configuration while forced at node 13. A first global bending mode was identified at 16.881 Hz. Many other "modes" were identified, as shown in the table on Figure 21, but there was considerable out-of-plane distortion in all of them. The measured frequency of 16.88 Hz is 2.4% lower than the predicted 17.3 Hz (reference Section 4). Although this difference is not great, the following explanations for this observation were investigated.

First, because coupling of local element bending and global truss bending had been observed during tube diagonal configuration tests, the effect of diagonal tension on bending frequency of the X-oriented (see Figure 4) tube members was calculated. The textbook method of calculating this effect is

$$f_b = f_a \sqrt{1 - P/P_c}$$

where

f_b is the bending frequency under axial load P

f_a is the bending frequency with no axial load (i.e., P = 0)

P is 40 cos 45° = 23.3 lb

and

P_c is the critical buckling load of the member.

Figure 20 Test Transfer Functions (Absolute Magnitude) for Box Truss with Tension Diagonals, No Freeplay, Shaker at Node 13, Y Motion

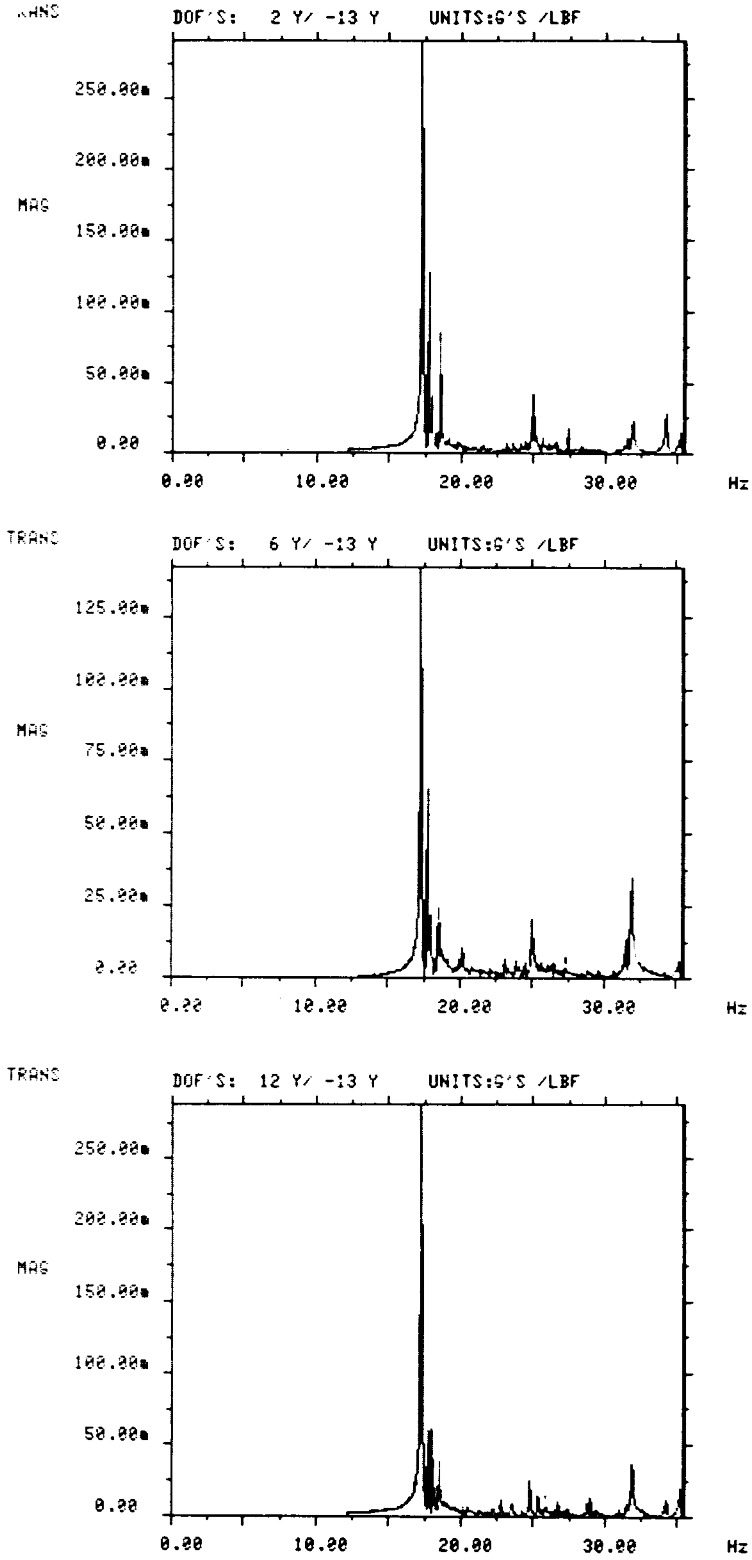

Figure 21 Measured Modes for Box Truss with Tension Diagonals and No Freeplay, Shaker at Node 13, Y Motion

MODAL FREQUENCY & DAMPING

MODE NO	FREQUENCY (HZ)	FREQUENCY (RAD/SEC)	DAMPING (HZ)	DAMPING (RAD/SEC)	DAMPING (%)
1	16.881	106.068	.169E-01	0.106	0.100
2	17.077	107.296	.166E-01	0.104	.973E-01
3	17.277	108.554	.143E-01	.901E-01	.830E-01
4	17.693	111.168	.166E-01	0.104	.938E-01
5	21.979	138.095	.962E-01	0.604	0.438
6	22.181	139.370	.253E-01	0.159	0.114
7	22.658	142.362	.197E-01	0.124	.868E-01
8	23.872	149.993	.205E-01	0.129	.860E-01
9	27.060	170.026	.373E-01	0.235	0.138
10	27.260	171.281	.959E-01	0.603	0.352
11	31.506	197.958	.386E-01	0.243	0.123
12	31.754	199.516	.443E-01	0.281	0.141
13	33.931	213.196	.468E-01	0.294	0.138

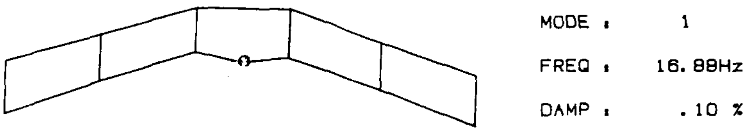

o Shaker Location

The critical buckling load was calculated to be 376.22 lb. As discussed in Section 4, the pinned-pinned frequency, f_a, of an element is 19.9 Hz, therefore

$$f_b = 19.9 \sqrt{1 - 28.3/376.22} = 19.1 \text{ Hz.}$$

This decrease of tube bending frequency is not sufficient to cause the observed decrease in global truss bending frequency. The second possible explanation investigated was that the diagonal preload caused a decrease in axial stiffness of the X-oriented (see Figure 4) tube members. This was thought possible because some curvature of the X members in the X-Z plane exists due to gravity. Axial compression loading from the tension diagonals increases this curvature to some extent. As the curvature increases, the end-loading stiffness becomes more dependent on bending stiffness and less on axial stiffness. No textbook solution to this problem could be found, so a finite element model of the beam with gravity-induced curvature was generated. An axial stiffness decrease of 0.5% was obtained from this model. This decrease was not significant and did not help explain the low observed first global truss bending frequency. Other attempts to explain the low frequency, such as a search for errors in the analytical model, and consideration of diagonal member stiffness decreases due to decrease of load carrying area at the thread of rod ends and center fittings flexibility, also failed.

Figures 22 and 23 present the respective test transfer function and modal (characteristics obtained for the clamped [no freeplay]) tension diagonal configuration while forced at node 14. Many poorly defined modes with out-of-plane motion were identified as indicated by the table in Figure 23. One typical example at 35.14 Hz is plotted. Again, local element bending coupled with global truss motion is suspected for these poor results. No mode shape having a second global truss mode shape was identified. In fact, no modes above 37.455 Hz were observed. No explanation for this outcome was found.

6.5 Test Results for Box Truss with Tension Diagonals and 1 mil Joint Freeplay

The comments on terminology (i.e., clamped vs. no freeplay and unclamped vs. 1 mil freeplay) made in Section 6.4 also apply here. This section presents test results of the unclamped configuration. Figures 24 and 25 present the respective test transfer functions and modal characteristics obtained for the unclamped (1 mil freeplay) tension diagonal configuration while forced at node 13. A first global bending mode was identified at 15.47 Hz. This deviation from the analytically predicted 17.3 Hz first global bending frequency was even greater than that observed in clamped (no freeplay) case discussed in Section 6.4.

Figure 22 Test Transfer Functions (Absolute Magnitude) for Box Truss with Tension Diagonals, No Freeplay, Shaker at Node 14, Y Motion

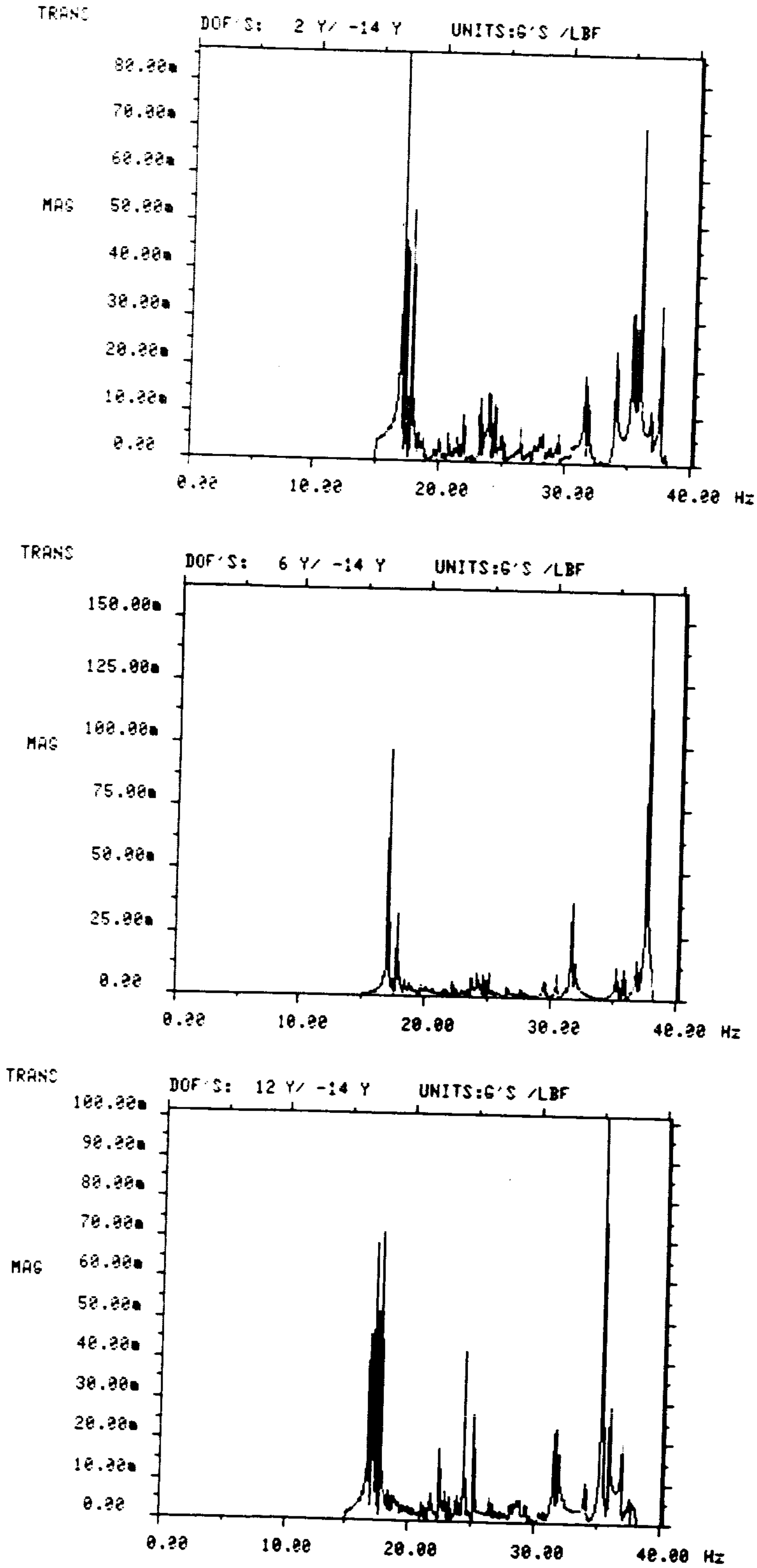

Figure 23 Measured Modes for Box Truss with Tension Diagonals and No Freeplay, Shaker at Node 14, Y Motion

MODAL FREQUENCY & DAMPING

MODE NO	FREQUENCY (HZ)	FREQUENCY (RAD/SEC)	DAMPING (HZ)	DAMPING (RAD/SEC)	DAMPING (%)
1	16.750	105.245	.358E-01	0.225	0.214
2	17.050	107.131	.233E-01	0.146	0.136
3	17.281	108.577	.158E-01	.991E-01	.913E-01
4	17.695	111.183	.104E-01	.655E-01	.589E-01
5	25.019	157.197	.327E-01	0.205	0.131
6	27.463	172.553	.359E-01	0.226	0.131
7	28.010	175.995	.583E-01	0.366	0.208
8	29.460	185.100	.441E-01	0.277	0.150
9	30.360	190.760	.450E-01	0.282	0.148
10	31.528	198.094	.435E-01	0.273	0.138
11	31.713	199.258	.452E-01	0.284	0.142
12	33.923	213.144	.518E-01	0.325	0.153
13	35.137	220.771	.247E-01	0.155	.703E-01
14	35.745	224.591	.281E-01	0.177	.786E-01
15	36.752	230.922	.384E-01	0.241	0.104
16	37.455	235.335	.272E-01	0.171	.727E-01

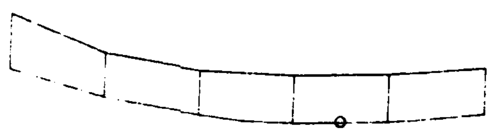

MODE : 13

FREQ : 35.14Hz

DAMP : .07 %

o Shaker Location

Figure 24 Test Transfer Functions (Absolute Magnitude) for Box Truss with Tension Diagonals, 1 mil Freeplay, Shaker at Node 13, Y Motion

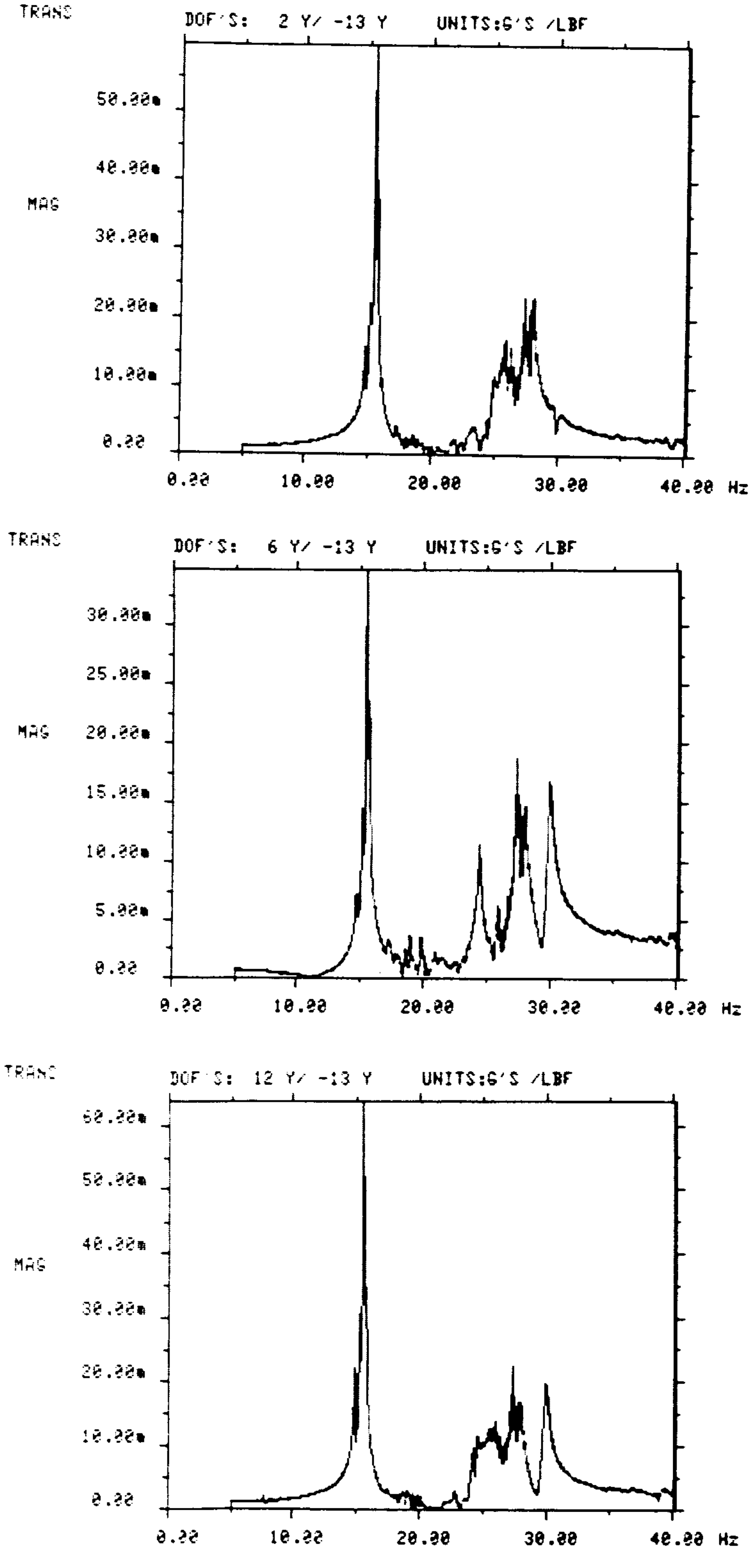

Figure 25 Measured Modes for Box Truss with Tension Diagonals and 1 mil Freeplay, Shaker at Node 13, Y Motion

MODAL FREQUENCY & DAMPING

MODE NO	FREQUENCY (HZ)	FREQUENCY (RAD/SEC)	DAMPING (HZ)	DAMPING (RAD/SEC)	DAMPING (%)
1	15.467	97.181	0.109	0.687	0.707
2	24.251	152.374	0.220	1.384	0.908
3	25.833	162.316	0.145	0.911	0.561
4	27.289	171.459	.663E-01	0.416	0.243
5	29.760	186.984	0.218	1.371	0.733

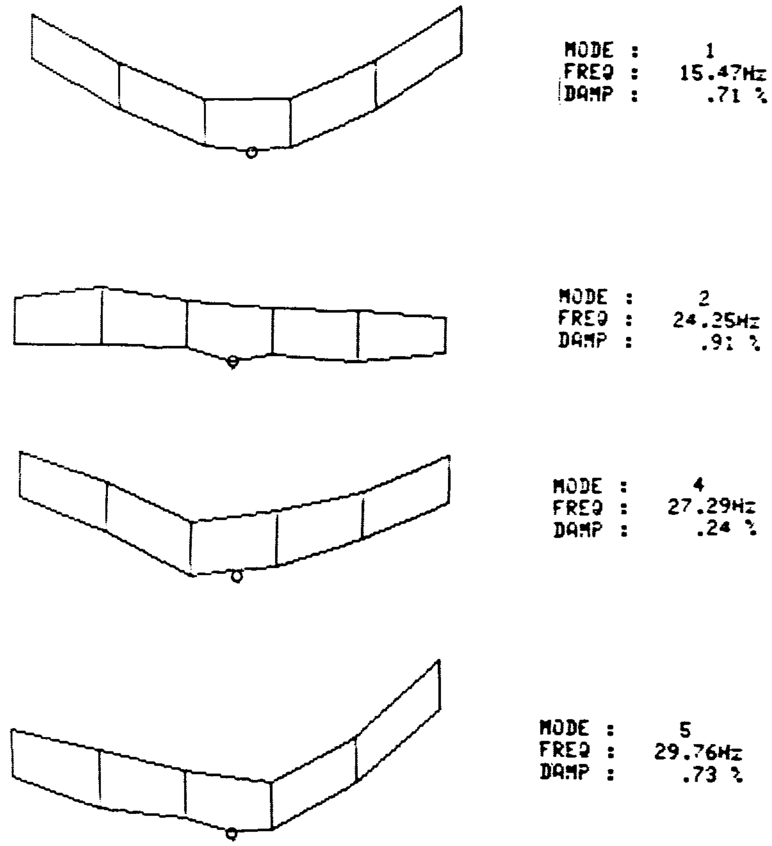

o Shaker Location

In addition to the low frequency first global bending mode, four other modes were identified as shown in the table in Figure 25. Plots of three of these are shown. Because of local global coupling, these shapes are not well defined. However, when the shaker was moved to node 14, similar modes were identified. Figure 27 presents these frequencies and mode shapes. (Figure 26 shows the corresponding test transfer functions.) Note that, with the exception of the 25.833 Hz and 48.751 Hz modes, the frequencies in the tables of Figures 25 and 27 compare quite well. And, although the mode shapes have obvious local distortions, the existence of global mode shapes, independent of shaker location is apparent from these plots. However, because of the local bending present in these modes, and because of the lack of sufficient instrumentation to measure the true kinetic energy distribution, the usual orthogonality checks to verify the quality of measured data could not be made.

Note that the apparent second global truss mode was identified at 49.75 Hz. This is not a dramatic decrease (-3.6%) from the 51.59 Hz mode identified for the tube diagonals configuration with 1 mil freeplay discussed in Section 6.3 (Figure 19).

Figure 26 Test Transfer Functions (Absolute Magnitude) for Box Truss with Tension Diagonals and 1 mil Freeplay, Shaker at Node 14, Y Motion

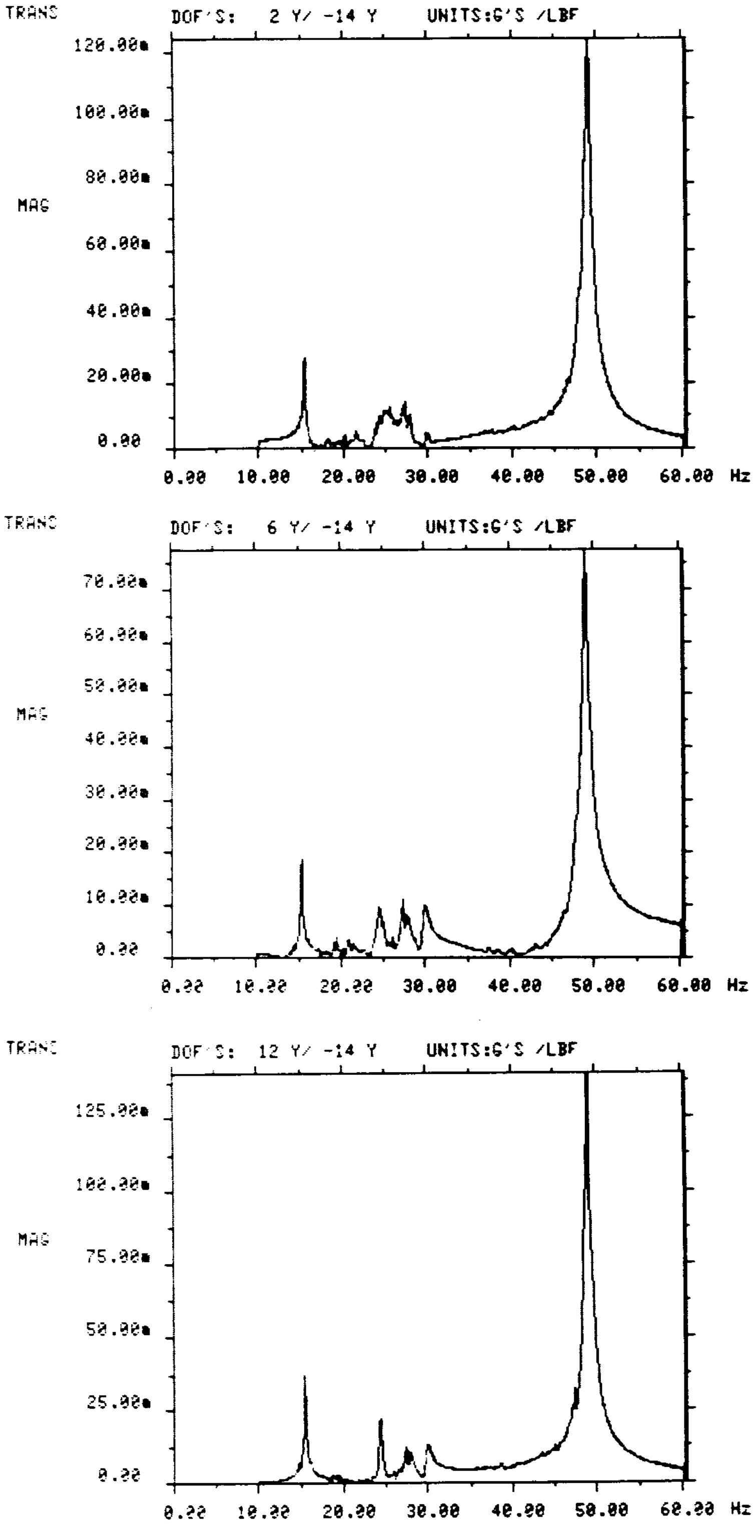

Figure 27 Measured Modes for Box Truss with Tension Diagonals and 1 mil Freeplay, Shaker at Node 14, Y Motion

MODAL FREQUENCY & DAMPING

MODE NO	FREQUENCY (HZ)	FREQUENCY (RAD/SEC)	DAMPING (HZ)	DAMPING (RAD/SEC)	DAMPING (%)
1	15.363	96.526	.925E-01	0.581	0.602
2	24.294	152.641	0.217	1.364	0.893
3	27.314	171.621	0.308	1.933	1.126
4	29.766	187.027	0.273	1.715	0.917
5	48.751	306.314	0.370	2.324	0.759

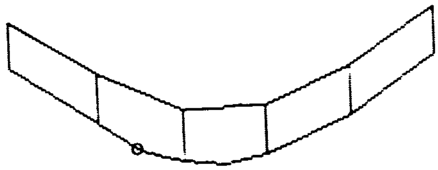

MODE : 1
FREQ : 15.36Hz
DAMP : .60 %

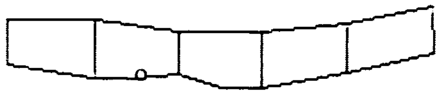

MODE : 2
FREQ : 24.29Hz
DAMP : .89 %

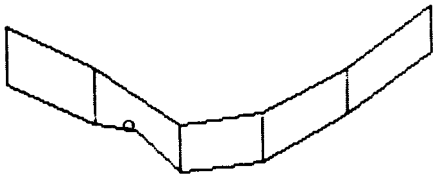

MODE : 3
FREQ : 27.31Hz
DAMP : 1.13 %

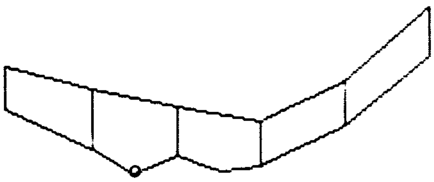

MODE : 4
FREQ : 29.77Hz
DAMP : .92 %

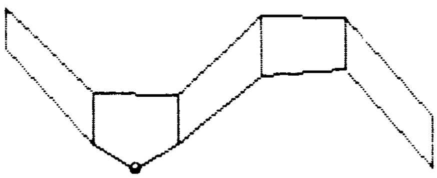

MODE : 5
FREQ : 48.75Hz
DAMP : .76 %

o Shaker Location

7.0 CONCLUSIONS AND RECOMMENDATIONS

7.1 Conclusions

The existence of local pinned-pinned bending frequencies of the 2-meter truss member in the range of global truss bending frequencies caused the introduction of a multitude of local/global bending modes. Because the shape and frequency of such modes depend on unknown and nonlinear effects, such as joint fixity and local bending frequency variations due to oscillating loads in global modes, analytical predictions are uncertain.

Theoretical/experimental correlation of such modes requires sufficient instrumentation to measure kinetic energy associated local member bending. The test configuration lacked sufficient instrumentation. Consequently, with the exception of the first global truss bending mode of the tube diagonal configuration, the primary value of the test results is to demonstrate the analytical modeling problems and associated control problems that arise when local/global coupling exists.

Quantification of the effect of joint freeplay was the only objective met. The tube diagonal configuration test data provided the information for this objective. 1-mil freeplay resulted in a drop in frequency. (First global truss bending mode was identified at 20 Hz without freeplay and at 17.72 Hz with freeplay.) This frequency shift was consistent with that predicted by the Martin Marietta Denver Aerospace-developed "Modal Freeplay" method, indicating that this method could be applied in future large space structures.

Although the measured frequency of the tension diagonal configuration was only 2.4% lower than that predicted neglecting tension effects, no explanation for this occurrence in terms of pretension effects, was found. Thus, the objective of assessing the effects of incorporating pretensioned diagonals was not met.

Damping is the least accurate parameter identified by curve fitting test transfer functions. Therefore, the uncertainties of the identified mode shapes and frequencies were of such magnitude as to preclude any conclusions regarding the effect of freeplay or preload on modal damping.

7.2 Recommendations

Future planning of large space structures tests should assure that the test article is designed so that local element bending frequencies are related to the global system frequencies by the same ratio as that expected in the operational space environment. This can be done by mass loading a test section of a large space structure or by increasing the member bending inertia of the test structure.

Conduct further investigations of the box truss test article, such as measuring actual stiffnesses of the steel diagonal rods and fittings, or performing parametric analyses to identify the conditions that produced the test-observed low fundamental global bending frequency.

APPENDIX A

FINITE ELEMENT MODEL INPUT DATA
FOR TUBE DIAGONALS CONFIGURATION

NODE LOCATIONS

NODE		X	Y	Z	
1	1	0.00	0.00	0.00	TRUSS
2	1	0.00	78.74	0.00	
3	1	78.74	78.74	0.00	
4	1	78.74	0.00	0.00	
5	1	157.48	0.00	0.00	
6	1	157.48	78.74	0.00	
7	1	236.22	78.74	0.00	
8	1	236.22	0.00	0.00	
9	1	314.96	0.00	0.00	
10	1	314.96	78.74	0.00	
11	1	393.70	78.74	0.00	
12	1	393.70	0.00	0.00	
13	1	472.44	0.00	0.00	
14	1	472.44	78.74	0.00	
15	1	551.18	78.74	0.00	
16	1	551.18	0.00	0.00	
17	1	629.92	0.00	0.00	
18	1	629.92	78.74	0.00	
19	1	708.66	78.74	0.00	
20	1	708.66	0.00	0.00	
21	1	787.40	0.00	0.00	
22	1	787.40	78.74	0.00	
23	1	787.40	79.74	-204.00	SUSPENSION WIRES
24	1	708.66	79.64	-204.00	
25	1	629.92	79.54	-204.00	
26	1	551.18	79.44	-204.00	
27	1	472.44	79.34	-204.00	
28	1	393.70	79.24	-204.00	
29	1	314.96	79.14	-204.00	
30	1	236.22	79.04	-204.00	
31	1	157.48	78.94	-204.00	
32	1	78.74	78.84	-204.00	
33	1	0.00	78.74	-204.00	
34	1	0.00	0.00	-204.00	
35	1	78.00	-0.05	-204.00	
36	1	157.48	-0.10	-204.00	
37	1	236.00	-0.15	-204.00	
38	1	314.00	-0.20	-204.00	
39	1	393.00	-0.25	-204.00	
40	1	472.00	-0.30	-204.00	
41	1	551.00	-0.35	-204.00	
42	1	629.00	-0.40	-204.00	
43	1	708.00	-0.45	-204.00	
44	1	787.00	-0.50	-204.00	

ELEMENT NO.	NODE a	NODE b	REF	AREA	POLAR AREA MOMENT OF INERTUA	SAINT VENANTS TORSION CONSTANT	AREA MOMENT OF INERTIA (LOCAL Z)	AREA MOMENT OF INERTIA (LOCAL Y)	SHEAR SHAPE FACTOR
401	1	2	4	0.1536	0.047268	0.03539	0.023634	0.023634	0.64
402	1	4	2	0.1536	0.047268	0.03539	0.023634	0.023634	0.64
403	2	4	1	0.1536	0.047268	0.03539	0.023634	0.023634	0.64
404	2	3	1	0.1536	0.047268	0.03539	0.023634	0.023634	0.64
405	3	4	2	0.1536	0.047268	0.03539	0.023634	0.023634	0.64
406	4	5	3	0.1536	0.047268	0.03539	0.023634	0.023634	0.64
407	3	5	4	0.1536	0.047268	0.03539	0.023634	0.023634	0.64
408	3	6	4	0.1536	0.047268	0.03539	0.023634	0.023634	0.64
409	5	6	4	0.1536	0.047268	0.03539	0.023634	0.023634	0.64
410	5	8	6	0.1536	0.047268	0.03539	0.023634	0.023634	0.64
411	6	8	5	0.1536	0.047268	0.03539	0.023634	0.023634	0.64
412	6	7	5	0.1536	0.047268	0.03539	0.023634	0.023634	0.64
413	7	8	6	0.1536	0.047268	0.03539	0.023634	0.023634	0.64
414	8	9	7	0.1536	0.047268	0.03539	0.023634	0.023634	0.64
415	7	9	8	0.1536	0.047268	0.03539	0.023634	0.023634	0.64
416	7	10	8	0.1536	0.047268	0.03539	0.023634	0.023634	0.64
417	9	10	8	0.1536	0.047268	0.03539	0.023634	0.023634	0.64
418	9	12	10	0.1536	0.047268	0.03539	0.023634	0.023634	0.64
419	10	12	9	0.1536	0.047268	0.03539	0.023634	0.023634	0.64
420	10	11	9	0.1536	0.047268	0.03539	0.023634	0.023634	0.64
421	11	45	10	0.1536	0.047268	0.03539	0.023634	0.023634	0.64
422	12	13	11	0.1536	0.047268	0.03539	0.023634	0.023634	0.64
423	11	13	12	0.1536	0.047268	0.03539	0.023634	0.023634	0.64
424	11	14	12	0.1536	0.047268	0.03539	0.023634	0.023634	0.64
425	13	14	12	0.1536	0.047268	0.03539	0.023634	0.023634	0.64
426	13	16	14	0.1536	0.047268	0.03539	0.023634	0.023634	0.64
427	14	16	13	0.1536	0.047268	0.03539	0.023634	0.023634	0.64
428	14	15	13	0.1536	0.047268	0.03539	0.023634	0.023634	0.64
429	15	16	14	0.1536	0.047268	0.03539	0.023634	0.023634	0.64
430	16	17	15	0.1536	0.047268	0.03539	0.023634	0.023634	0.64
431	15	17	16	0.1536	0.047268	0.03539	0.023634	0.023634	0.64
432	15	18	16	0.1536	0.047268	0.03539	0.023634	0.023634	0.64
433	17	18	16	0.1536	0.047268	0.03539	0.023634	0.023634	0.64
434	17	20	18	0.1536	0.047268	0.03539	0.023634	0.023634	0.64
435	18	20	17	0.1536	0.047268	0.03539	0.023634	0.023634	0.64
436	18	19	17	0.1536	0.047268	0.03539	0.023634	0.023634	0.64
437	19	20	18	0.1536	0.047268	0.03539	0.023634	0.023634	0.64
438	20	21	19	0.1536	0.047268	0.03539	0.023634	0.023634	0.64
439	19	21	20	0.1536	0.047268	0.03539	0.023634	0.023634	0.64
440	19	22	20	0.1536	0.047268	0.03539	0.023634	0.023634	0.64
441	21	22	20	0.1536	0.047268	0.03539	0.023634	0.023634	0.64
442	12	45	9	0.1536	0.047268	0.03539	0.023634	0.023634	0.64

ALUMINUM TUBE PROPERTIES

$E = 10^7$ psi, $G = 3.75(10)^6$ psi

DENSITY = .100 lb/in^3

ELEMENT NO.	NODE a	NODE b	AREA AT a	AREA AT b
42	22	23	0.0491	0.0491
43	19	24	0.0491	0.0491
44	18	25	0.0491	0.0491
45	15	26	0.0491	0.0491
46	14	27	0.0491	0.0491
47	11	28	0.0491	0.0491
48	10	29	0.0491	0.0491
49	7	30	0.0491	0.0491
50	6	31	0.0491	0.0491
51	3	32	0.0491	0.0491
52	2	33	0.0491	0.0491
53	1	34	0.0491	0.0491
54	4	35	0.0491	0.0491
55	5	36	0.0491	0.0491
56	8	37	0.0491	0.0491
57	9	38	0.0491	0.0491
58	12	39	0.0491	0.0491
59	13	40	0.0491	0.0491
60	16	41	0.0491	0.0491
61	17	42	0.0491	0.0491
62	20	43	0.0491	0.0491
63	21	44	0.0491	0.0491

SUSPENSION WIRE PROPERTIES

$E = 1.4(10)^5$ psi

DENSITY = .0386 lb/in^3

CONCENTRATED WEIGHT AT NODES 3 THROUGH 20 = 1.22 lbs

CONCENTRATED WEIGHT AT NODES 1, 2, 21, 22 = .97 lbs

APPENDIX B

FINITE ELEMENT MODEL INPUT DATA
FOR TENSION DIAGONALS CONFIGURATION

NODE LOCATIONS

NODE		X	Y	Z	
1	1	0.00	0.00	0.00	TRUSS
2	1	0.00	78.74	0.00	
3	1	78.74	78.74	0.00	
4	1	78.74	0.00	0.00	
5	1	157.48	0.00	0.00	
6	1	157.48	78.74	0.00	
7	1	236.22	78.74	0.00	
8	1	236.22	0.00	0.00	
9	1	314.96	0.00	0.00	
10	1	314.96	78.74	0.00	
11	1	393.70	78.74	0.00	
12	1	393.70	0.00	0.00	
13	1	472.44	0.00	0.00	
14	1	472.44	78.74	0.00	
15	1	551.18	78.74	0.00	
16	1	551.18	0.00	0.00	
17	1	629.92	0.00	0.00	
18	1	629.92	78.74	0.00	
19	1	708.66	78.74	0.00	
20	1	708.66	0.00	0.00	
21	1	787.40	0.00	0.00	
22	1	787.40	78.74	0.00	
23	1	787.40	79.74	-204.00	SUSPENSION WIRES
24	1	708.66	79.64	-204.00	
25	1	629.92	79.54	-204.00	
26	1	551.18	79.44	-204.00	
27	1	472.44	79.34	-204.00	
28	1	393.70	79.24	-204.00	
29	1	314.96	79.14	-204.00	
30	1	236.22	79.04	-204.00	
31	1	157.48	78.94	-204.00	
32	1	78.74	78.84	-204.00	
33	1	0.00	78.74	-204.00	
34	1	0.00	0.00	-204.00	
35	1	78.00	-0.05	-204.00	
36	1	157.48	-0.10	-204.00	
37	1	236.00	-0.15	-204.00	
38	1	314.00	-0.20	-204.00	
39	1	393.00	-0.25	-204.00	
40	1	472.00	-0.30	-204.00	
41	1	551.00	-0.35	-204.00	
42	1	629.00	-0.40	-204.00	
43	1	708.00	-0.45	-204.00	
44	1	787.00	-0.50	-204.00	
45	1	393.70	39.37	0.00	BAY CENTERS
46	1	39.37	39.37	0.00	
47	1	118.11	39.37	0.00	
48	1	196.85	39.37	0.00	
49	1	275.59	39.37	0.00	
50	1	354.33	39.37	0.00	
51	1	433.07	39.37	0.00	
52	1	511.81	39.37	0.00	
53	1	590.55	39.37	0.00	
54	1	669.29	39.37	0.00	
55	1	748.03	39.37	0.00	

ELEMENT NO.	NODE a	NODE b	REF.	AREA	POLAR AREA MOMENT OF INERTIA	SAINT VENANTS TORSION CONSTANT	AREA MOMENT OF INERTIA (LOCAL Z)	AREA MOMENT OF INERTIA (LOCAL Y)	SHEAR SHAPE FACTOR
201	1	2	4	0.1536	0.047268	0.03539	0.023634	0.023634	0.64
202	1	4	2	0.1536	0.047268	0.03539	0.023634	0.023634	0.64
204	2	3	1	0.1536	0.047268	0.03539	0.023634	0.023634	0.64
205	3	4	2	0.1536	0.047268	0.03539	0.023634	0.023634	0.64
206	4	5	3	0.1536	0.047268	0.03539	0.023634	0.023634	0.64
208	3	6	4	0.1536	0.047268	0.03539	0.023634	0.023634	0.64
209	5	6	4	0.1536	0.047268	0.03539	0.023634	0.023634	0.64
210	5	8	6	0.1536	0.047268	0.03539	0.023634	0.023634	0.64
212	6	7	5	0.1536	0.047268	0.03539	0.023634	0.023634	0.64
213	7	8	6	0.1536	0.047268	0.03539	0.023634	0.023634	0.64
214	8	9	7	0.1536	0.047268	0.03539	0.023634	0.023634	0.64
216	7	10	8	0.1536	0.047268	0.03539	0.023634	0.023634	0.64
217	9	10	8	0.1536	0.047268	0.03539	0.023634	0.023634	0.64
218	9	12	10	0.1536	0.047268	0.03539	0.023634	0.023634	0.64
220	10	11	9	0.1536	0.047268	0.03539	0.023634	0.023634	0.64
221	11	45	10	0.1536	0.047268	0.03539	0.023634	0.023634	0.64
222	12	13	11	0.1536	0.047268	0.03539	0.023634	0.023634	0.64
224	11	14	12	0.1536	0.047268	0.03539	0.023634	0.023634	0.64
225	13	14	12	0.1536	0.047268	0.03539	0.023634	0.023634	0.64
226	13	16	14	0.1536	0.047268	0.03539	0.023634	0.023634	0.64
228	14	15	13	0.1536	0.047268	0.03539	0.023634	0.023634	0.64
229	15	16	14	0.1536	0.047268	0.03539	0.023634	0.023634	0.64
230	16	17	15	0.1536	0.047268	0.03539	0.023634	0.023634	0.64
232	15	18	16	0.1536	0.047268	0.03539	0.023634	0.023634	0.64
233	17	18	16	0.1536	0.047268	0.03539	0.023634	0.023634	0.64
234	17	20	18	0.1536	0.047268	0.03539	0.023634	0.023634	0.64
236	18	19	17	0.1536	0.047268	0.03539	0.023634	0.023634	0.64
237	19	20	18	0.1536	0.047268	0.03539	0.023634	0.023634	0.64
238	20	21	19	0.1536	0.047268	0.03539	0.023634	0.023634	0.64
240	19	22	20	0.1536	0.047268	0.03539	0.023634	0.023634	0.64
241	21	22	20	0.1536	0.047268	0.03539	0.023634	0.023634	0.64
242	12	45	9	0.1536	0.047268	0.03539	0.023634	0.023634	0.64
343	2	46	3	0.02761165	0.00012134	0.00012134	0.00006067	0.00006067	0.90
344	3	46	2	0.02761165	0.00012134	0.00012134	0.00006067	0.00006067	0.90
345	1	46	4	0.02761165	0.00012134	0.00012134	0.00006067	0.00006067	0.90
346	4	46	1	0.02761165	0.00012134	0.00012134	0.00006067	0.00006067	0.90
347	3	47	6	0.02761165	0.00012134	0.00012134	0.00006067	0.00006067	0.90
348	6	47	3	0.02761165	0.00012134	0.00012134	0.00006067	0.00006067	0.90
349	4	47	5	0.02761165	0.00012134	0.00012134	0.00006067	0.00006067	0.90
350	5	47	4	0.02761165	0.00012134	0.00012134	0.00006067	0.00006067	0.90
351	6	48	7	0.02761165	0.00012134	0.00012134	0.00006067	0.00006067	0.90
352	7	48	6	0.02761165	0.00012134	0.00012134	0.00006067	0.00006067	0.90
353	5	48	8	0.02761165	0.00012134	0.00012134	0.00006067	0.00006067	0.90
354	8	48	5	0.02761165	0.00012134	0.00012134	0.00006067	0.00006067	0.90
355	7	49	10	0.02761165	0.00012134	0.00012134	0.00006067	0.00006067	0.90
356	10	49	7	0.02761165	0.00012134	0.00012134	0.00006067	0.00006067	0.90
357	8	49	9	0.02761165	0.00012134	0.00012134	0.00006067	0.00006067	0.90
358	9	49	8	0.02761165	0.00012134	0.00012134	0.00006067	0.00006067	0.90
359	10	50	11	0.02761165	0.00012134	0.00012134	0.00006067	0.00006067	0.90
360	11	50	10	0.02761165	0.00012134	0.00012134	0.00006067	0.00006067	0.90
361	9	50	12	0.02761165	0.00012134	0.00012134	0.00006067	0.00006067	0.90
362	12	50	9	0.02761165	0.00012134	0.00012134	0.00006067	0.00006067	0.90
363	11	51	14	0.02761165	0.00012134	0.00012134	0.00006067	0.00006067	0.90
364	14	51	11	0.02761165	0.00012134	0.00012134	0.00006067	0.00006067	0.90
365	12	51	13	0.02761165	0.00012134	0.00012134	0.00006067	0.00006067	0.90
366	13	51	12	0.02761165	0.00012134	0.00012134	0.00006067	0.00006067	0.90
367	14	52	15	0.02761165	0.00012134	0.00012134	0.00006067	0.00006067	0.90
368	15	52	14	0.02761165	0.00012134	0.00012134	0.00006067	0.00006067	0.90
369	13	52	16	0.02761165	0.00012134	0.00012134	0.00006067	0.00006067	0.90
370	16	52	13	0.02761165	0.00012134	0.00012134	0.00006067	0.00006067	0.90
371	15	53	18	0.02761165	0.00012134	0.00012134	0.00006067	0.00006067	0.90
372	18	53	15	0.02761165	0.00012134	0.00012134	0.00006067	0.00006067	0.90
373	16	53	17	0.02761165	0.00012134	0.00012134	0.00006067	0.00006067	0.90
374	17	53	16	0.02761165	0.00012134	0.00012134	0.00006067	0.00006067	0.90
375	18	54	19	0.02761165	0.00012134	0.00012134	0.00006067	0.00006067	0.90
376	19	54	18	0.02761165	0.00012134	0.00012134	0.00006067	0.00006067	0.90
377	17	54	20	0.02761165	0.00012134	0.00012134	0.00006067	0.00006067	0.90
378	20	54	17	0.02761165	0.00012134	0.00012134	0.00006067	0.00006067	0.90
379	19	55	22	0.02761165	0.00012134	0.00012134	0.00006067	0.00006067	0.90
380	22	55	19	0.02761165	0.00012134	0.00012134	0.00006067	0.00006067	0.90
381	20	55	21	0.02761165	0.00012134	0.00012134	0.00006067	0.00006067	0.90
382	21	55	20	0.02761165	0.00012134	0.00012134	0.00006067	0.00006067	0.90

ALUMINUM TUBE PROPERTIES

$E = 10^7$, $G = 3.75(10)^6$

DENSITY = .100 lb/in^3

STEEL DIAGONAL PROPERTIES

$E = 3(10)^7$, $G = 10^7$

DENSITY = .272 lb/in^3

ELEMENT NO.	NODE a	NODE b	AREA AT a	AREA AT b
42	22	23	0.0491	0.0491
43	19	24	0.0491	0.0491
44	18	25	0.0491	0.0491
45	15	26	0.0491	0.0491
46	14	27	0.0491	0.0491
47	11	28	0.0491	0.0491
48	10	29	0.0491	0.0491
49	7	30	0.0491	0.0491
50	6	31	0.0491	0.0491
51	3	32	0.0491	0.0491
52	2	33	0.0491	0.0491
53	1	34	0.0491	0.0491
54	4	35	0.0491	0.0491
55	5	36	0.0491	0.0491
56	8	37	0.0491	0.0491
57	9	38	0.0491	0.0491
58	12	39	0.0491	0.0491
59	13	40	0.0491	0.0491
60	16	41	0.0491	0.0491
61	17	42	0.0491	0.0491
62	20	43	0.0491	0.0491
63	21	44	0.0491	0.0491

SUSPENSION WIRE PROPERTIES

$E = 1.4(10)^5$ psi

DENSITY = .0386 lb/in^3

CONCENTRATED WEIGHT AT NODES
3 THROUGH 20 = 1.295 lbs

CONCENTRATED WEIGHT AT NODES
1, 2, 21, 22 = 1.163 lbs

CONCENTRATED WEIGHT AT NODES
45 THROUGH 55 = .231 lbs

Standard Bibliographic Page

1. Report No. NASA CR-4039	2. Government Accession No.	3. Recipient's Catalog No.
4. Title and Subtitle Dynamic Testing of a Two-Dimensional Box Truss Beam		5. Report Date January 1987
		6. Performing Organization Code D6-44238-5
7. Author(s) Charles W. White		8. Performing Organization Report No. MCR-86-575
9. Performing Organization Name and Address Martin Marietta Denver Aerospace P. O. Box 179, Mail Stop M0486 Denver, Colorado 80201		10. Work Unit No.
		11. Contract or Grant No. NAS1-17551
12. Sponsoring Agency Name and Address National Aeronautics and Space Administration Washington, D.C. 20546		13. Type of Report and Period Covered Contractor Report
		14. Sponsoring Agency Code 506-62-23

15. Supplementary Notes

Langley Technical Monitor: U. M. Lovelace
Final Report

16. Abstract

Testing to determine the effects of joint freeplay and pretensioning of diagonal members on the dynamic characteristics of a two-dimensional box truss beam was conducted. The test article was ten bays of planar truss suspended by long wires at each joint. Each bay measured 2 meters per side. Pins of varying size were used to simulate various joint freeplay conditions. Single-point random excitation was the primary method of test. The rational fraction polynomial method was used to extract modal characteristics from test data.

A finite element model of the test article was generated from which modal characteristics were predicted. These were compared with those obtained from test. With the exception of the fundamental mode, correlation of theoretical and experimental results was poor. It was determined that the poor correlation was caused by the resonant coupling of local truss member bending modes with global truss beam modes. This coupling introduced many modes in the frequency range of interest whose frequencies were very sensitive to joint boundary conditions. It was concluded that local/global coupling must be avoided in the frequency range where accurate modal characteristics are required.

17. Key Words (Suggested by Authors(s)) Dynamic Testing, Theoretical/Experimental Correlation, Joint Modeling Effects, Modal Strain Energy Review	18. Distribution Statement Unclassified - Unlimited Subject Category 18		
19. Security Classif.(of this report) Unclassified	20. Security Classif.(of this page) Unclassified	21. No. of Pages 66	22. Price A04

For sale by the National Technical Information Service, Springfield, Virginia 22161

NASA-Langley, 1987